Critical Compilation of Surface Structures Determined by Ion Scattering Methods

Philip R. Watson

Department of Chemistry, Oregon State University, Corvallis, Oregon 97331-4003

Received October 13, 1988; revised manuscript received April 24, 1989

This review critically compiles all surface structures derived by ion scattering techniques reported in the refereed literature prior to January 1988. They are compared with the more extensive low-energy electron diffraction database reported previously [J. Phys. Chem. Ref. Data **16**, 953 (1957)]. These investigations cover all types of surfaces including clean and adsorbate-covered metal, semiconductor, and other nonmetallic substrates. The important experimental and theoretical aspects of such investigations have been extracted into easily understood tabular form supplemented by many figures and ancillary tables and complete references. It is hoped that this compilation will provide a valuable resource both for the surface science specialist and for those nonspecialists in other areas who need surface crystallographic data.

Key words: critically reviewed data; ion scattering; channelling; blocking; surface crystallography; surface structure.

Contents

List of Tables

List of Figures

1. Introduction

1.1. Background

urfaces play an increasingly important role in technol- n the construction of microelectronics circuits, the ac- f catalysts, and in the areas of metallurgy, tribology, rrosion. Many of the most dramatic advances in these have resulted from the application of the methods of e science.

he geometrical arrangement of atoms in a surface or ed layer is perhaps the single most basic item of infor- n that we need in order to understand the behavior of faces of materials. From the surface crystallography, all other understanding flows. Thus, a knowledge of e structure is a prerequisite for studies of electronic ties. Without surface crystallographic information, attempts to define adsorption and reactions on surfaces are critically hindered.

A number of techniques that are sensitive to the atomic geometry of surfaces have been developed, using electron, photon, and ion probes. The most widely-used of these has been low-energy electron diffraction (LEED), which was the subject of a previous critical compilation.[1] Of the other methods, ion scattering studies have provided the most information on surface crystallography.

Unlike the LEED literature, which contains several lists of derived structures, there have been few attempts to compile an overview of the results from ion scattering, critical or otherwise. However, several interesting reviews exist. The most comprehensive is that of van der Veen[2] which provides a good review of the principles of high- and medium-energy scattering, and discussion of applications to surfaces and interfaces up to 1984. The present compilation provides a greater depth of detail of a wider range of investigations, including low-energy studies, and brings the listing up to date. In particular we provide a survey of surface structural results that has been critically examined as to the accuracy and internal consistency of the quoted results. The present compilation summarizes in detail the ion-scattering surface crystallography literature in a condensed, but easily accessible, database. In addition, the results are discussed and compared with existing LEED structures. It is hoped that this survey will be a valuable resource not only for specialists in surface science, but also for workers in other disciplines that need surface structural data to understand and extend their work, but lack the time or resources to evaluate the complex and interrelating factors that contribute to the derivation of a structure quoted in the literature.

1.2. Organization and Scope

The body of the review is organized as follows. First we very briefly review the basic aspects of ion scattering experiments to orient those readers not familiar with this topic. More complete accounts can be found in the reviews referred to therein. Next we examine in some detail the various components that go into a surface structural determination by these methods and attempt to establish criteria that would give us a reasonable degree of confidence in the derived result.

The compilation of surface structures is presented in the form of a large table (Table 2), showing the most important experimental and theoretical parameter values and a brief description of the results of the study. Further discussion of some of the reported structures follows in Sec. 5, and is divided into three sections covering: (1) Clean surfaces of metals and alloys, (2) adsorbate-covered metal surfaces, and (3) nonmetallic surfaces, clean and adsorbate covered. Each discussion section contains a number of accompanying notes, figures, and ancillary tables. These serve to amplify and clarify the brief descriptions given in the main table. Where possible we compare the ion scattering results with well-established LEED structures. However, in the interests of brevity, we do not fully discuss the LEED data, only the best-accepted results. Readers who require more informa-

tion on LEED surface crystallographic structures are urged to refer to the previous compilation,[1] and references therein.

The temporal scope of this review covers surface structures determined by ion scattering methods reported in the refereed literature since the inception of modern investigations, roughly 1975, until January 1988.

The scope has also been deliberately limited in other ways. The first is that in order to ensure the reliability of the compilation, only papers appearing in normal peer-reviewed journals were considered; articles published in unrefereed conference proceedings or society bulletins are not included. Secondly, the review is restricted as much as is feasible to "true surface structures"—that is, to studies that result in the finding of the atomic coordinates of atoms in the first few atomic layers of a solid. This approach provides a natural continuity with the previous compilation. Hence, investigations dealing with the structure of buried interfaces, or defects in thin films, are excluded. As these problems are becoming increasingly common goals in ion scattering, particularly for channelling experiments, this exclusion may lead some readers to the mistaken impression that the review is missing recent references. Thirdly, where the same group of investigators has reported several times on the same structural problem (perhaps in increasing levels of detail), the results have been consolidated into one table entry. However, in such cases all the references are supplied.

2. Surface Structural Techniques

2.1. Introduction

There are many techniques available that are sensitive to one or another structural aspect of a surface. For the purposes of this review we shall not use the term "structure" to mean a completely determined geometry, in the sense that an x-ray crystallographer might understand the term. Surface crystallography has not advanced to that highly automated level of development. Rather we interpret "structure" in the broadest sense to mean a report of a surface geometry that may be fragmentary and incomplete, but still advances our understanding of the system.

The previous compilation[1] was concerned with the large database of LEED structures. Other surface structural techniques have been applied to a smaller range of materials. Of these, the ion-scattering spectroscopies, in their low-, medium-, and high-energy versions, have supplied the major fraction of the reported structures.

2.2. Ion Scattering Methods

Surface structure determinations using ion scattering have tended to become grouped into three types, depending upon the energy regime of the probe ion—low, medium, or high. The distinction between medium- and high-energy scattering, is in many ways an artificial one, based more upon different experimental requirements than substantial differences in the physics of the interactions.

Low-energy ion scattering (LEIS) experiments generally use ion energies of up to a few keV, and can be distinguished from the medium-energy counterpart (MEIS), in which energies are measured in 10's or 100's of keV. The distinction between medium- and high-energy scattering (HEIS) is less firm on energetic grounds. High-energy experiments usually employ MeV beams, but may drop substantially below this, while some MEIS experiments may use energies as high as 300 keV. However, the spirit of the experiments, and the apparatus used, is usually rather different for the two regimes. For the purposes of this review, we shall make the following arbitrary energetic dividing lines between the three scattering methods: (1) Low energy (LEIS): <10 keV; (2) Medium energy (MEIS): 10 keV–250 keV; (3) High energy (HEIS): >250 keV.

The physics of the interactions of ions with surfaces is simpler, at least in the energy ranges for HEIS and MEIS, than that for low-energy electrons. Furthermore, the ion scattering techniques directly determine atomic positions in real, rather than reciprocal, space. The interpretation of HEIS and MEIS spectra are more straightforward than the corresponding LEED data. As a result useful information, such as adsorbate locations, can frequently be found almost by inspection. For the most accurate HEIS and MEIS crystallographic work, significant calculations are needed, which can rival those necessary in LEED.

In the following sections we will very briefly review the essentials of ion scattering experiments in each regime.

2.2.a. High-Energy Ion Scattering (HEIS)

High-energy ion scattering is a surface-sensitive variant of the frequently used technique, Rutherford backscattering spectrometry (RBS). When the first attempts to apply RBS to surface structure determinations were performed about 15 years ago, the method already had a long history as a thin-film analytical tool.[3] A number of excellent reviews of HEIS exist,[2,4–9] although most concentrate on experimental methods and theory, rather than a comprehensive list of results.

In a typical HEIS experiment a collimated MeV beam of ions, often He or H, is incident on a planar sample and a solid-state nuclear particle detector measures the scattered particles. If the ion beam is carefully aligned along a major symmetry direction of the crystal, most of it is then channeled in this direction by the atom strings of the solid; the ions cannot approach close enough to undergo large-angle Rutherford scattering. As a result the signal from the bulk of the solid is dramatically reduced. The surface atoms are always accessible to the ion beam, and so the surface peak (SP) becomes clearly separated in the energy spectrum.

When ions scatter from the surface layer of the solid they project a "shadow-cone" within which scattering from atoms in deeper layers is suppressed. In an ideal lattice, the size of the SP is related to the relative sizes of the two-dimensional thermal vibration amplitude, and the radius of the shadow cone. One of the great strengths of HEIS is that the response of the SP to different surface structures can be predicted in a simple geometrical manner.

Obtaining detailed crystallography involves calculating the SP expected for a particular postulated surface structure. The nuclear backscattering probability is determined by a Monte Carlo approach[9–12] in which a large number of trajectories of ions in the crystal are followed. The interaction potential is frequently of the screened Coulomb type due to

oliere.[13] The other main input to the calculations are the brational amplitudes of the surface and near-surface oms, which are not known *a priori*. Recent work has exored the effect of correlated atomic motions on the SP.[14] ıe lack of information on vibrational properties of surface oms may ultimately limit the accuracy of structural deterination by ion scattering methods.

The form in which data is collected and analyzed is ually of two main types: (1) The SP intensity is measured a certain channeling direction, and at a number of ion ergies, and the resulting experimental SP/energy curve ted to calculations. (2) A "rocking-curve" consisting of e SP intensity as a function of small changes of angle about e channelling direction is compared with theory.

The extraction of the SP intensity is sensitive to the ethod of background subtraction.[11]

The angular and/or energy data is then compared with lculations for various assumed geometries in a trial-andror process, monitored often by a reliability (R-) factor. In ntrast to LEED, and most other techniques, ion scattering oss sections can be measured and calculated in absolute, ther than relative, units. Hence, there is less need in ion attering for the complex R-factors that have been necesry in LEED to account for the arbitrariness of the ordiıte. Typically, simple, statistically justifiable, R-factors ıve been used for HEIS (Table 1); they are all based on ot-mean-square differences between experimental and eoretical quantities. The factors differ in the use of experiental weighting factors (RWIS[18] and RIS[17]), and normalition (RSQ)[16] as shown below:

$$\mathrm{RSQ} = \frac{1}{N}\left[\sum_{i=1}^{N}\left[Y_{th} - Y_{ex}\right]^2\right]^{1/2}$$

$$\mathrm{RIS} = \frac{100}{N}\left[\sum_{i=1}^{N}\left(\frac{\left[Y_{th} - Y_{ex}\right]}{Y_{ex}}\right)^2\right]^{1/2}$$

$$\mathrm{RWIS} = 100\,\frac{1}{N}\left[\sum_{i=1}^{N}\left(\frac{\left[Y_{th} - wY_{ex}\right]}{wY_{ex}}\right)^2\right]^{1/2}$$

ıere Y_{th} and Y_{ex} are the calculated and experimental SP ılds, N the number of data points, and w a weighting factor ɔse to 1 that takes account of experimental errors.

2.2.b. Medium-Energy Ion Scattering (MEIS)

Ion scattering in the medium energy range has been extensively developed and reviewed by Dutch workers.[2,19-21] It shares a similar conceptual base, and employs many of the same theoretical approaches as HEIS.

The critical component that most clearly differentiates most MEIS and HEIS studies is the use of "blocking" of the exiting backscattered particle in addition to channeling of the incoming ion. If a backscattering atom is located below the surface, then the outgoing scattered ion may be blocked along its exit track by another atom, resulting in a decrease in the SP in that direction.

If the sample and detector are accurately set up in "double alignment", that is, with the ion beam incident along a channeling direction, and the detector on a blocking direction, then changes in interlayer spacings can be measured from the tilt angle of the surface blocking cone with respect to the bulk axis.

The usual method of data presentation in MEIS is the surface blocking pattern. Here the intensity of the SP, for a given channeling direction, is measured about one or more blocking directions. The position and shape of the blocking minima can then be compared with calculations for assumed surface structures.[22-24]

The use of R-factors in MEIS studies has increased lately. There appears to be trend to use factors that are more securely based in statistical theory; two popular R-factors are[24,25]:

$$\mathrm{R1}v = \frac{1}{vs}\sum_{i=1}^{N}\left|wY_{ex} - Y_{th}\right|$$

$$\mathrm{R2}v = \frac{1}{vs^2}\sum_{i=1}^{N}\left[wY_{ex} - Y_{th}\right]^2$$

where, s is the standard deviation in data values $Y(ex)_i$, N is the number of data points, v is the number of degrees of freedom = (N − the number of parameters to fit), and w is a weighting factor

2.2.c. Low-Energy Ion Scattering (LEIS)

The low-energy ions employed in LEIS interact so strongly with solid materials that scattering is almost com-

Table 1. Reliability (R-) factors used for ion scattering crystallography.

R-factor	Application	Form[a]	Ref.
RSQ	HEIS	R.M.S. Th-Exp	16
RIS	HEIS,MEIS	Normalized RSQ	17
RWIS	HEIS	Weighted RIS	18
R1v	MEIS	Mean Th-Exp	25
R2v	MEIS	Similar to RWIS	31

[a] for more detail see text

pletely confined to the topmost surface layer. As a result, ion scattering spectroscopy (ISS) has found considerable use as a surface analytical tool.[26] As a surface structural probe, LEIS shares many of the same phenomena as MEIS or HEIS, in particular the use of blocking. But LEIS is also distinctly separated from HEIS and MEIS experiments in that quantitative analysis is much less straightforward due to a poorer understanding of the interaction potential, and a lack of knowledge of the probability of neutralization of the scattered ion. A number of reviews of various aspects of LEIS are in the literature.[27-30]

In LEIS, the kinematic relations for the energy of the scattered projectile remain unchanged from higher energies, at least under the assumption of two-particle interactions. The intensity of the peak in the scattered ion spectrum depends upon, in addition to the surface density of the scattering atom, the differential scattering cross section and the neutralization probability. The former has been generally calculated assuming a screened Coulomb potential, in a similar manner to HEIS. The neutralization probability is a more difficult problem, although the basic physical processes are known.[32] The neutralization problem has been attacked in several ways; alkali metal beams,[33,34] time-of-flight mass spectrometry,[35,36] and neutral reionization.[37]

The manner in which LEIS has been used to provide surface structural information falls into two main classes:

(1) simple experiments which yield crude, but often useful information. Thus the relative position of two atomic species in a surface, e.g., subsurface versus adsorbed, can sometimes be found by observing the ratio of their LEIS signals.

(2) More sophisticated studies where quantitative structural information is found from data obtained at several different incidence and exit angles. The surface unit cell can be directly imaged using multichannel plate detectors.[38]

The latter types of investigations make use of the concept of the shadow cone and surface blocking as outlined earlier. If an atom falls within the shadow cone of another, then it cannot contribute to the scattered intensity. Thus, by measuring the scattered intensity from an adsorbate, for instance, at various azimuthal exit angles, the shadowing effect of substrate atoms can pinpoint the adsorbate location. For inert gas ions, the analysis is complicated by trajectory-dependent neutralization effects.[32] While the use of alkali ions reduces the neutralization probability, multiple scattering effects often require comparisons with extensive Monte Carlo codes.[39,40]

One of the most powerful applications of LEIS has been the development of impact collision ion scattering spectroscopy (ICISS).[41,42] In this mode the scattering angle is set as close to 180° as possible. Accordingly, only ions having undergone head-on collisions (an impact parameter near to zero) are observed, reducing the effects of multiple scattering. At some critical incident polar angle, a sharp increase in the scattered intensity occurs. Each critical angle is geometrically related to the distance between the atoms in a particular row, and so, if the shape of the shadow cone is known, we can determine a number of interatomic distances by measurement of several critical angles. To avoid the use of a theoretical shadow cone, some workers have used expe mental cones previously measured on a surface of kno structure as a self-calibrating procedure.[29]

Most LEIS experiments do not involve extensive co parisons of experimental data with calculations made f assumed surface structures, but rather derive structural formation from such experimental data as critical angles. a result R-factors do not seem to be in use in these type scattering studies.

In the low-energy regime, scattering from a well- dered surface produces characteristic energy and angu distributions. As thermal vibrations act as a quasistatic s face disordering on the time-scale of the ion–surface inter tion, they can have an influence on the spectra, and any rived structural results. Most authors have not attempted build in different Debye temperatures for surface atoms their interpretations, but there does appear to be an incre ing tendency for investigators to allow this as another str tural parameter to be fitted.[43,44]

3. Evaluation Criteria

Determining a surface structure using ion scattering volves surface preparation, collection of the scattering d and derivation of the structure, possibly involving calcu tions for a particular postulated surface structure and co parison with the experimental data. Each of these stages associated with it certain problems that may affect the r ability of the result and may involve judgements that may open to more than one interpretation.

Hence a proper critical evaluation of a surface crysta graphic study involves a consideration of many different tors, which may have complex interrelationships, that affect our confidence in the reported result.

The methodology for critically evaluating ion scat ing crystallographic data will focus principally on the n critical areas of the technique, the collection of data comparison of theory with experiment. Most workers h used tested and reliable computational schemes, hence exact method of calculation is not often a strong determir of reliability.

Given the many diverse components that go into a c plete study, and the many factors that can influence the ability of a given result, it is difficult to come up with s simple numerical index that would signify a "good" "bad" structure. The most realistic solution to providi confidence level for a given result is to draw up a lis criteria which would define a very reliable study. In s instances such a criterion might indeed be numerica contamination level in percent of a monolayer, or the n ber of datasets used in a comparison of theory and ex ment. In other instances we might be able to give a ye answer to questions like "Is a reliability-factor used?" Sc times it may only be possible to reveal unquantifiable mi ings about some aspect of the procedures—for inst doubts as to a careful avoidance of disturbing effects suc beam damage.

Therefore, we will now examine each step of a ty ion scattering experiment and discuss the factors that a the results. The criteria that are developed here form

s for the columns reported in the main database table and ıld be read before using the table for a proper under- ding of their meaning and function

3.1. Experimental Aspects

3.1.a. Surface Preparation

The preparation of the surface under study is such a lamental part of any surface crystallography experiment incumbent upon us to make a critical examination of the :ribed procedures.

The first goal of any surface science experiment is to ɔare the surface under consideration in the required ı. The single-crystal sample is usually cut from a rod or e, oriented and polished using standard metallographic ıods, and mounted on a manipulator. With care the ori- tion of the polished crystal should be within 1°, or less, of desired plane. Few workers, however, explicitly state they check that the x-ray face, as found from a back- ction Laué photograph, is parallel to the polished opti- ace. This can be easily done using a small He–Ne align- t laser. As the metallographic techniques for preparing a hed crystal slice of a particular orientation are standard edures, we assume here that the sample is oriented to in 1°, unless the authors state otherwise.

The contamination and damage introduced during the ng and polishing processes is usually removed by clean- ıe surface to below some acceptable level of contamina- using thermal, chemical, or ion bombardment tech- :s. Chemisorbed structures can then be obtained by :ption. Analytical techniques such as Auger electron roscopy (AES)[45] or x-ray photoelectron spectroscopy S)[46] can reveal adatom concentrations at the level of a ɔercent of a monolayer coverage, and form useful ad- techniques. Of course the ion scattering spectra them- ;, or surface nuclear reaction analysis (NRA)[47] can be to monitor surface composition, making the inclusion :se other analytical techniques not strictly necessary.

The question of what constitutes a clean surface is of e a vexed one, and can depend very much on the sys- ınd the requirements and sensitivity of the experiment. it is much more difficult to produce a truly clean iron ınium surface, than a copper or gold surface. Or a sur- :econstruction might be turned on or inhibited by small nts of contamination. Nevertheless, we suggest the use (generous) figure of 5% of a monolayer to represent ɔer bound to an acceptable contamination level in ordi- :ircumstances.

)f necessity, LEED surface crystallography studies ɔeen carried out on well-defined highly ordered sur- Due to the local nature of the ion scattering process, :striction disappears. However, many ion scattering s have been performed on systems that are known to ɔrdered structures; in some cases this is merely as- to be the case. It is most reassuring to know that the nental data is in fact from the same structure that nethods have studied. For this to be, some means has :ovided to assess the surface order. The natural tool to LEED optics present in the sample chamber, to pro- vide a qualitative check on the symmetry and order of the surface under examination. In the absence of any well-defined quantitative measure of surface crystallinity, workers generally rely on a visual judgement of a low background coupled with small, sharp diffraction spots to indicate a well-crystallized surface.

Thus, in the area of surface preparation we can formulate a number of criteria for effective preparation:

(1) Is the contamination level below 5% of a monolayer? Are actual spectra shown, or peak ratios noted, to back-up this value?

(2) Are ancillary analytical methods used, and do they corroborate the ion scattering data?

(3) Is the surface highly crystalline? Are photographs of LEED patterns provided?

To be fully assured of adequate surface preparation we should be able to give an affirmative answer to all these questions. In fairness, however, it would be sufficient for an author to refer to a previous paper in which these details have been covered.

3.1.b. Data Collection and Surface Damage

Data collection in ion scattering can involve the measurement of a large number of scattering spectra taken at different incidence and scattering angles. Hence data collection times can be rather long and the question of surface damage becomes one of importance.

The number of surface atoms that are displaced or sputtered by an incident ion varies greatly with the substrate and the ion energy. High-energy ions, such as MeV protons, displace only about 10^{-3} substrate atoms per incident ion. This is a low rate of damage production; for a typical HEIS experimental beam dose of 10^{15} ions per cm^2, only $\sim 10^{12}$ atoms, or $<1\%$ of a monolayer, are displaced in the near surface region. On the other hand, ions in the LEIS energy range can have sputtering yields greater than unity. In this case experiments must be performed at low dosages to avoid significant damage to the surface. It is certainly appropriate for authors, particularly at the lower ion energies, to quote the beam dose to which the sample was exposed.

It is particularly reassuring to find that closely similar sets of experimental data have been measured from more than one separately prepared sample. In general, however, we must acknowledge that preparing and cleaning are sufficiently difficult that such duplication of data may not be easy.

Based on the above arguments we can suggest the following criteria for effective data collection: (1) The beam dose should be reported, and should result in $<1\%$ of a monolayer damage to the surface. (2) Ideally, identical data should have been obtained from more than one sample.

3.2. Structure Determination

The derivation of a surface structure from ion scattering data depends greatly upon the detail and precision desired in the final structure. It can be as simple as comparing the size of two spectral features, or as difficult as a multiparameter fit of much angular data with complex Monte Carlo calculations for many different assumed structures.

However, there are a number of considerations that apply to at least most experimental configurations and levels of sophistication. These concern the amount of data available, the procedure for comparing experiment and theory, and the difficulty of finding unique structural solutions. We suggest below a number of criteria in this area, and proceed to explain and justify them. These are: (1) At least two independent set of data should be available. (2) Where appropriate, a numerical reliability factor or index should be used. (3) Several surface structural models should be examined, possibly including changes in more than one interlayer spacing, registry shifts, and surface vibrational amplitudes. (4) Any estimated error should be consistent with the demonstrated procedures.

3.2.a. Amount of Experimental Data

One of the most noticeable aspects of the ion scattering literature are the variations in the amount and nature of the data collected in different studies. The effect is partly historical; many early studies fit a small amount of experimental data to find a surface structure, but as experimentalists have become more proficient, there is a tendency to collect more extensive datasets.

Obviously there exists a linkage between the total amount of data used and the reliance that we can place on the structural result. It is difficult to suggest any amount of data that represents an unacceptably small dataset; there appears to be little or no consensus on this point among practitioners. In the tables compiled in this review we have reported or made a best estimate, not always a trivial procedure in some cases, the number of incidence angles used, and the size of the total dataset. This latter quantity could be made up of a number of angular scans taken at different energies, or a number of azimuthal detection angles, or some combination. In some cases only "Many" suffices.

Despite the disclaimer announced above, it seems appropriate to at least attempt to define a minimum dataset size that would inspire confidence in the reader. We suggest that a minimum of two different experimental conditions, i.e., angle or energy combinations, should be measured.

3.2.b. Comparison of Theory and Experiment

In many cases the experimental data is compared with corresponding calculations to decide which model surface structure best fits the measured data. Many workers in the early days of the technique used visual methods of comparison. While the eye has excellent sensitivity for distinguishing small details between a pair of calculated and observed curves, it is very difficult to assess the cumulative fit of many such pairs and it can be hard to obtain agreement between different judges.

It is clearly desirable to have the work of comparing many sets of experimental and theoretical data done in an objective and consistent manner by computer. The lack of agreement between different workers as to what constitu a good reliability factor means that is difficult to find ma studies that use exactly the same index. Hence it is not usu ly possible to use R-factor values to distinguish between c fering results found by different groups. However, R-fact do have a very important role to play in finding an interna consistent best-fit structure for a particular set of experim tal data. The use of such quantitative measures does all for a consistent evaluation of competing structural mod and of comparison of results from one laboratory to anoth

A problem that frequently arises in this context is th changes in a nonstructural parameter, particularly surfa vibrational amplitudes, and changes in a structural quanti such as a bond length, are coupled together. Thus, the val of the structural parameter producing the best fit betwe the observed and calculated data may change if the value the nonstructural parameter is altered. Hence it is importa for authors to state whether such effects have been inves gated.

We note here that it appears to be common in the i scattering literature for authors to suppress powers of ten presenting R-factor topographs. This can make comparis between studies carried out on different laboratories di cult.

Another difficulty is that of deciding when enough d ferent structural models have been tested to give us con dence that we are not resting in some local minimum of t parameter space, but are truly at the global minimum of t system. Once again, we cannot, in reality, assign any ha and fast numbers to this criterion. Its role will be essentiall negative one; in cases where, for instance, only a very sm number of models were tested, it would have an impact in t total estimation of the reliability of the determination.

A final possible criterion refers to the error limits their results quoted by some authors—thus a bond leng may be reported as being within 0.1 Å of a certain value. Th value may result from the step used in the variation of structural parameter such as a layer spacing or bond lengt or may be derived from an interpolation of a grid of R-fact results. Here this criterion will again be used in a negati sense—that is, it will be noted if the quoted error does n appear to be consistent with the data and procedures d scribed in the paper.

3.3. Overall Assessment of Reliability

. Having enunciated several criteria for estimating t degree of confidence we find in a particular structure det mination, it remains to try to find a way to wrap all the different factors into one overall assessment of the con dence level of the structure. As discussed earlier, this is ve difficult to do because of the varied nature of the differe criteria and the lack of a numerical basis for distinguishi conflicting results.

Accordingly, this critical compilation presents t reader with a rather complete picture of a study in a ve condensed form in Table 2. It is arranged so as to allow t reader to easily and quickly find a structure. Thus the read will quickly be able to tell to form a judgement as to t extent that a particular study has fulfilled the criteria su

ested above. Table 2 is followed in Sec. 5 by an expanded iscussion with numerous figures and ancillary tables.

4. Surface Structure Compilations

4.1. Organization and Nomenclature

Table 2 presents the surface structure compilations. It ontains values of the pertinent experimental and theoretical arameters discussed earlier in a concise, but easily under- tood form. Also the table shows structural and nonstruc- ıral parameters derived from the experimental data. In ad- ition, there are also short comments on interesting points of :chnique, and simple descriptions of the derived structures ıat cannot be easily shown numerically. As some structures re too complex to be easily summarized in this manner, ıore detailed discussion can be found in Sec. 5.

The Table is organized so that a particular structure can : readily found. The entries are arranged with the following iorities: (1) Alphabetically by substrate.

(2) Numerically by the surface plane Miller indices, ., (100) before (110) before (111).

(3) Alphabetically by adsorbate, when present.

(4) Size of the unit cell, i.e., (1×1) before (2×1) be- re (2×2). Here we arbitrarily assign p(2×2) higher pri- ity than c(2×2).

(5) Chronologically by date of publication.

Below are listed explanations of some of the symbols ed as table headings and abbreviations and acronyms that ıy be encountered in the body of the tables. When an entry ntains a dash (-), this indicates that this information was t specified. A query (?) indicates that the value of the rameter in question was discussed but not clearly defined.

bstrate (*Subs.*):

The chemical symbol of the substrate.

face (*Surf.*):

The Miller indices of the surface under investigation.

orbate (*Ads.*):

The identity of any adsorbate present.

ucture (*Struct.*):

The symmetry of the surface structure present, using ıdard surface crystallographic notation.

erence (*Ref.*):

The reference number of the study as given in Section

hod (*Meth.*):

The type of ion scattering experiment performed.

a Collection (*Data Coll.*):

The manner in which the data was collected. The acro- ıs used are (see text for details):

CMA—cylindrical mirror (electrostatic) analyzer
ESA—electrostatic analyzer (sector, or toroidal)
ICISS—impact collision ion scattering spectroscopy
IAC—induced Auger channeling
LEIBAD—low-energy ion bombardment angular dis- ıtions
LERS—low-energy recoil spectroscopy
MC—multichannel plates
NRECOIL—nuclear recoil spectrometry
SB—surface barrier detector
TOF—time-of-flight mass spectrometry
TC—transmission channeling

Ion:

The identity of the projectile ion(s).

Energy (*E*):

The ion energy in keV.

Dose:

The maximum ion dose seen by the area of the crystal under investigation in ions/m^2.

Contamination Level (*Cont. level*):

The reported level of surface contamination in mono- layers, or other specified units. L(ow) indicates an unspeci- fied "clean" state.

Other Techniques (*Other tech*):

Other techniques that were used during the investiga- tion to monitor, e.g, surface composition (AES, XPS, etc.) or surface structure (LEED). Acronyms used here are:

AES—Auger electron spectroscopy.
LEED—low-energy electron diffraction
MEED—medium-energy electron diffraction
NRA—nuclear reaction analysis
PIXE—proton-induced x-ray emission
RBS—Rutherford backscattering spectroscopy.
UPS—ultraviolet photoelectron spectroscopy
WF—work function
XPS—x-ray photoelectron spectroscopy
XRD—x-ray diffraction

When spectra are reproduced then S appears in parentheses.

Number of Angles (*Angs.*):

The number of angles of incidence at which data was taken.

Data Sets (*Data*):

The total number of datasets measured (all angles and energies—see text).

Temperature (*Temp.* (*K*)):

The temperature at which the experiment was per- formed in degrees K.

Calculation (*Calcs.*):

The method of calculation used; by reference.

R-factor (*R-*):

Only the type of R-factor is quoted because of doubts over suppressed powers of ten. For R-factor definitions, see Sec. 2.2.

Debye (*K*):

The value of the surface Debye temperature (in K) used in calculations. In some cases the parallel (∥) and per- pendicular (⊥) components are given separately.

d-B:

The value of the interlayer spacing in the bulk material in Å.

d-0:

The value of the distance of an overlayer from the cen- ter of the topmost layer substrate in the normal direction (Å). Error in parentheses when given. In parentheses is giv- en the adsorption site symmetry as below: (see Sec. 5.2 for more detail)

4F = 4-fold coordinate site, e.g., FCC(100)
3F = 3-fold coordinate site, e.g., FCC(111)

TABLE 2. Surface structures determined by ion scattering.

Subs.	Surf.	Ads.	Struct.	Ref.	Data Meth.	Data coll.	Ion	E(keV)	Dose (m^{-2})	Cont. level	Other tech.	Angs.	Data	Temp. (K)	Calcs.	R	Debye (K)	d-B (Å)	d-C (Å)	d-1 (%)	d-2 (%)	Comments
Ag	110	—	(1×1)	17	HEIS	SB	He	400	—	L	LEED/AES	3	3	300	7	RIS	149	1.445	—	−7.8(2.5)	+4.3(2.5)	—
Ag	110	—	(1×1)	25	MEIS	ESA/MC	H	53,98	?	L	LEED/AES	3	4	300	2	Riv	150	1.445	—	−9.5(2.0)	+6.0(2.5)	—
Ag	110	O	(2×1)	48	LEIS	ESA	He	0.6	—	L(S)	LEED/AES	2	2	—	48	—	—	1.445	0.0 (2F-L)	—	—	O in surface channels in bridge site, close to coplanar with top layer Ag atoms.
Ag	111	Au		49	HEIS	SB	He	1000	—	L	LEED/AES	2	4	300	—	—	—	2.359	—	—	—	Closely epitaxial layer by layer growth. Au mainly (90%) in FCC sites.
Au	110	—	(1×2)	16	HEIS	SB	He	200–1600	?	L	LEED/AES	2	4	100,293	11	RSQ	110	1.442	—	+/−17	—	Confirm missing-row model with lateral displacements in 2nd layer 0.12 Å (100 K), 0.18 Å (298 K).
Au	110	—	(1×2)	50	HEIS	SB	He	—	—	—	XRD	2	2	100	7	—	—	1.442	—	—	—	Missing-row structure with lateral pairing in 2nd row of 0.12 Å, possibly outward relaxation.
Au	110	—	(1×2)	51	LEIS	ESA	K,He	0.6	—	L	—	2	2	300	53	—	—	1.442	—	—	—	Data does not support (i) distorted hexagonal overlayer, (ii) unrelaxed missing-row or (iii) high degree of disorder
Au	110	—	(1×2)	52	MEIS	SB	He	300	—	L	LEED/AES	2	2	—	9	—	—	1.442	—	—	—	Data agree best with large expansion model [54], or small contraction and 2nd layer expansion [55]. Could not match line widths.
Au	110	—	(1×2)	56	MEIS	ESA/MC	H	65,200	—	—	LEED	3	3	—	2,7	—	130	1.442	—	−18	+4	Three samples. Confirm missing-row structure with 3rd layer buckling. Difficult to distinguish pairing effects in 2nd layer from vibrational effects.
Au	110	—	(1×2)	57	LEIS	ESA/TOF	Ne,Na	?	?	L	LEED	1	4+	300–800	57	—	—	1.442	—	−13.9(4.8)	—	Extension of [57]. Took data at several temperatures. Favor missing-row structure with contraction. Followed phase transition to (1×1).
Au	110	—	(1×2)	58	LEIS	ICISS/TOF	Ne	?	?	—	—	6	6	—	—	—	—	1.442	—	−0.4(6.9)	—	Agrees with missing-row model.
Au	110	—	(1×2)	59	LEIS	—	K	0.6	—	—	—	2	2	—	53	—	—	1.442	—	−7.3(2.7)	—	Use data from [55]. Lateral pairing displacement in 2nd layer <0.10 Å.
Au	110	—	(1×2)	60	MEIS	ESA/MC	H	65,180	—	L	LEED	2	2	—	—	—	—	1.442	—	−8	—	Missing-row structure.
C(dia)	111	—	p(2×1)	61	MEIS	ESA	H	99	6E+21	—	LEED	2	5	300	2	R2v	—	0.515	—	—	—	Formed after 950 °C anneal. Data compatible with pi-bonded chain model with dimerization parallel to chains [62].
C(dia)	111	H	(1×1)	61	MEIS	ESA	H	99	6E+21	—	LEED	2	5	300	2	R2v	—	0.515	—	<10	—	H-saturated surface. Small relaxation agrees with LEED [63].
CaF_2	111	—	—	153	HEIS	—	He	1500	6E+19	L	—	2	2	—	—	—	—	—	—	—	—	Film grown by MBE on Si(111) at 700 °C. Films less than 200 nm thick were strained.
Cu	100	Au	c(2×2)	64	LEIS	CMA	He	1	?	L	LEED/AES/UPS	1	1	—	—	—	—	1.807	—	—	—	Ordered surface resembles Cu3Au(100); 50% Au in top layer.
Cu	100	O	c(2×2)	32	LEIS	CMA	He	1	—	L	LEED/AES	2	2	625	32	—	—	1.807	—	—	—	Needed to include ion-atom neutralization. Difficult to distinguish 2F bridge from 4F hollow adsorption sites.
Cu	100	O	c(2×2)	65	LEIS	ESA	Ne	1	—	—	—	Many	Many	—	—	—	—	1.807	—	—	—	No reconstruction; 2 sites involved, possibly 2F/4F. At higher coverages (√2×2√2)R45 structure involves O penetrating subsurface

Subs.	Surf.	Ads.	Struct.	Ref.	Meth.	Data coll.	Ion	E(keV)	Dose (m^{-2})	Chem. level	Other tech.	Angs.	Data	Temp. (K)	Calcs.	R	Debye (K)	d_{12} (Å)	d_{23} (Å)	Δ_1 (%)	Δ_2 (%)	Comments
Cu	110	—	(1×1)	66	HEIS	SB	He	300	6E + 19	L	LEED/AES	2	2	300	11	RWIS	250	1.278	—	− 5.3	+ 3.3	Agrees with LEED [66b].
Cu	110	—	(1×1)	67	LEIS	ICISS	Li	5	?	L	LEED/AES	3	3	300	68	—	258	1.278	—	− 10(5)	—	—
Cu	110	—	(1×1)	69	MEIS	ESA/MC	H	100	4E + 20	L	LEED/AES	2	2	323	11	RWIS	205	1.278	—	− 7.5(1.5)	+ 2.5(1.5)	—
Cu	110	O	(2×1)	70	LEIS	NRECOIL	Ne,F_2O	4	?	L	LEED	4	8	—	—	—	—	1.278	(2F − L)	—	—	O atoms in bridge sites as before but Cu atoms in missing-row reconstruction.
Cu	110	O	(2×1)	71	HEIS	SB	He	200–2000	—	L	LEED/AES	2	10	300	11	RWIS	250	1.278	—	See Notes	—	No agreement with missing-row model. Best agreement with buckled surface model with every 2nd [001] row displaced out by 0.27(05) Å, whole 2nd layer shifts out by 0.06(03) Å. Adsorption at 100 K.
Cu	110	O	(2×1)	67	LEIS	ICISS	Li	5	?	L	LEED/AES	3	3	300	68	—	258	1.278	—	+ 25	− 10	200L O_2/100 °C for 5 min. Data consistent with missing, but not buckled-row, reconstruction.
Cu	110	O	—	72	LEIS	ESA	Ne	3–5	—	—	Many	Many	Many	—	10	—	—	1.278	− 0.((2F − L)	—	—	Little evidence for reconstruction. O in long bridge site.
Cu	110	O	—	29	LEIS	ICISS	Na	2	—	L	LEED/AES/WF	5	5	—	—	—	—	1.278	—	—	—	10–5 mbar/s O_2 at room temp. and anneal 370 °C min. Favor missing row model.
Cu	111	O	—	73	LEIS	ICISS	He	2	—	L	LEED/AES/WF	3	3	300	—	—	—	2.087	—	—	—	Surface reconstructed with Cu atoms displaced by 0.3 Å. No subsurface O.
Cu	410	—	(1×1)	74	LEIS	ESA	Ar,Ne	8–11	?	—	—	4	8	540	74	—	—	—	—	—	—	Showed terraces 4 atoms wide separated by 1-atom steps.
Cu	410	O	—	75	LEIS	ESA	Ne,Na	5	?	—	—	2	3	—	75	—	147	—	—	—	—	O at hollow sites of step edges.
Cu	16,1,1	—	(1×1)	76	MEIS	SB	He	Several	?	C,O < 3%	LEED/AES/NRA	Many	Many	300	76	—	350	—	—	− 3*	—	*in ⟨100⟩ direction. No step-edge relaxation. O adsorption reverses sign of Cu relaxation and induces facetting.
Cu_3Au	100	—	(1×1)	77	LEIS	TOF	Ne	5,9.5	—	—	LEED/AES	2	3	Several	—	—	—	—	—	—	—	50% Au in top layer; 0% in 2nd.
Fe	100	—	(1×1)	78	LEIS	TOF	Ne	9.5	—	Some C,N	LEED/AES	3	Many	300	10	—	—	1.433	O	—	—	4% Sn/Fe alloy stoichiometry retained if sputter < 400 °C. No reconstruction.
Fe	100	O	(1×1)	79	LEIS	ESA/TOF	Ne	5	—	L	—	2	2	300	10	—	—	1.433	0.56(05)(4F)	—	—	15L O_2/room temp than anneal at 700 K/15 min. gave ordered 1ML coverage.
Fe	100	Sn	(2×2)	80	LEIS	TOF	Ne	9.5	—	—	LEED/AES	2	4	300	40	—	—	1.433	—	—	—	Segregated from 1.7% Sn-Fe alloy by heating 600 °C/1 hr. Top layer all Sn in Fe sites, 2nd layer all Fe. New LEED (2×2) may be due to adsorbed Sn.
GaAs	100	—	c(4×4)	81	HEIS	SB	He	2000	1.5E + 20	—	LEED/PIXE	—	—	—	9,11	—	333,291	1.414	—	—	—	Grown by MBE. Significant lateral displacements of 1st layer As and subsurface strain.
GaAs	100	H	(1×1)	81	HEIS	SB	He	2000	1.5E + 20	—	LEED/PIXE	—	—	—	9,11	—	333,291	1.414	—	—	—	H_2/hot filament; surface is bulklike.
GaAs	110	—	(1×1)	82a	HEIS	SB	He	2000	1.5E + 20	L	LEED/AES	2	2	—	9,11	—	333,291	1.999	—	—	—	Annealed 630 °C. Ga, As have small lateral displacements; data consistent with relaxed-bond, 7° Ga–As chain rotation model.
GaAs	110	—	(1×1)	83	MEIS	ESA	H	50,100	1E + 20	L	LEED	2	4	300	84	R2/	—	1.999	—	—	—	Ga–As chains rotate through 29°, conserving bond lengths. Attribute disagreement with [82a] to high annealing temperature.

TABLE 2. Surface structures determined by ion scattering (continued).

Subs.	Surf.	Ads.	Struct.	Ref.	Data Meth.	Data coll.	Ion	E(keV)	Dose (m^{-2})	Cont. level	Other tech.	Angs.	Data	Temp. (K)	Calcs.	R	Debye (K)	d-B (Å)	d-0 (Å)	d-1 (%)	d-2 (%)	Comments
GaAs	110	Au,Pd	(1×1)	12b	HEIS	SB	He	2000	1.5E + 20	L	MEED/AES	2	2	300	9,12	—	333,291	1.999	—	—	—	Pd, but not Au, affects substrate structure substantially.
GaSb	110	—	(1×1)	15b	MEIS	ESA/MC	He	174	6E + 18	L	—	1	1	300	2	R2v	222,136	2.163	—	See Notes	—	Bond lengths conserved, Ga–Sb bond rotated by 29°. Thermal vibrational amplitudes of surface atoms increased by a factor of 1.5.
InAs	110	—	(1×1)	15a	MEIS	ESA/MC	He	174	6E + 18	L	—	1	1	300	2	R2v	—	2.142	—	See Notes	—	Similar structure to GaAs and GaSb with with 30° rotation.
Ir	110	—	(1×2)	40	MEIS	ESA/MC	H	65,180	—	L	LEED	1	1	—	—	—	—	1.352	—	− 10	—	Missing-row structure.
LaB_6	100	—	(1×1)	16	LEIS	ESA	He	1	—	L	LEED/XPS	1	1	—	—	—	—	—	—	—	—	Surface terminated by La; in case of SmB_6 Coverage by Sn less complete.
LaB_6	111	—	(1×1)	17	LEIS	ESA	He	1	—	L	LEED/XPS/UPS	3	3	300	—	—	—	1.20	—	—	—	La atoms at surface may be relaxed outwards.
Mo	111	—	(1×1)	18	LEIS	ESA	Li	1	?	Sm.C	LEED/AES	10	10	300	40	—	—	0.907	—	− 18(2)	+ 4(4)	—
Ni	100	—	(1×1)	19	MEIS	ESA/SB	H	52,98	1E + 19	L	LEED/AES	2	3	370	40	—	285	1.762	—	− 3.2	+ 1	Surface Debye temperature significantly increased relative to bulk.
Ni	100	D	—	90	HEIS	TC	He	800	?	L	LEED/AES/RBS	3	3	120	91	—	375	1.762	0.5(0.1)(4F)	—	—	Grown epitaxially on NaCl(100) and floated onto Nisupport. Used NRA to detect D.
Ni	100	O	(2×1)	100	LEIS	ESA	Ar,Ne	6	—	—	?	4	12	300	—	—	—	1.246	< 0.5(2F-L)	—	—	Missing-row model favored; O in long-bridge sites.
Ni	100	O	c(2×2)	92	LEIS	—	He	1	—	L	LEED	1	1	300	—	—	—	1.762	0.9(0.2)	—	—	O in 4F hollow site.
Ni	100	O	c(2×2)	19	MEIS	ESA/SB	H	52,98	1E + 19	L	LEED/AES	2	2	370	89	—	285	1.762	0.86(4F)	+ 5.2	—	—
Ni	100	S	c(2×2)	93	LEIS	ICISS	Ne	5	6E + 18	—	LEED	2	2	—	—	—	—	1.762	1.40(0.05)	—	—	—
Ni	100	Te	c(2×2)	90a	HEIS	TC	He	2000	—	L	LEED/AES/RBS	2	2	170	91	—	375	1.762	1.9(0.1)(4F)	—	—	Grown on NaCl(100). Te in 4F hollow sites.
Ni	110	—	(1×1)	94	MEIS	ESA	H	160–200	—	L	—	2	2	300	—	—	—	1.246	—	O	—	—
Ni	110	—	(1×1)	95	MEIS	ESA	H	100	3E + 20	L	—	1	1	300	—	—	—	1.246	—	− 4(1)	—	With 0.33ML O, d-l is + 1(1).
Ni	110	—	(1×1)	96	HEIS	SB	He	300	?	L	LEED/AES	2	2	298	11	RWIS	325	1.246	—	− 4.8(1.7)	+ 2.4(1.2)	—
Ni	110	—	(1×1)	97	MEIS	SB	H	100	?	L	LEED/AES	2	2	—	—	—	—	1.246	—	− 4(1)	—	—
Ni	110	—	(1×1)	98	MEIS	ESA/SB	H	110	?	L	LEED/AES	3	3	300	9,12	RWIS	395	1.246	—	− 9.0(1.0)	+ 3.5(1.5)	Previous discrepancies with LEED attributed to chanliness problems.
Ni	110	C,O	—	99	HEIS	SB	D	1200	—	—	—	2	2	300	—	—	—	1.246	(2F–L)	—	—	O and C in long-bridge positions. Identified by nuclear reactions.
Ni	110	O	(2×1)	101	MEIS	ESA/MC	H	100	2E + 19	L	LEED/AES	2	2	370	22	—	—	1.246	—	—	—	3 min at 1×10^{-9} Torr oxygen for best LEED pattern. Estimate that ~ 50% of surface covered by missing-row O-induced reconstruction.
Ni	110	O	(2×1)	102	MEIS	IAC	H	150	1E + 19	L	—	3	3	300	?	—	260	1.246	2.5(1.5)	—	—	2L O_2 at 350 K for 0.5ML. Prefer saw-tooth rather than missing-row model. O atoms in long-bridge site.
Ni	110	O	(2×1)	103	LEIS	ICISS	Na	2	1E + 17	L	LEED/AES	3	3	—	—	—	—	1.246	0.25(2F-L)	—	—	Missing-row structure; O in ⟨001⟩ bridge site.
Ni	110	O	(2×1)	104	LEIS	NRECOIL	Ne	2	?	L	—	4	4	< 350	—	—	—	1.246	0.23(2F-L)	—	—	O in long-bridge site in ⟨001⟩ direction.

Subs.	Surf.	Ads.	Struct.	Ref.	Meth.	Data coll.	Ion	E(keV)	Dose (m^{-2})	Cont. level	Other tech.	Angs.	Data	Temp. (K)	Calcs.	k	Debye (K)	d-B (Å)	d-O (Å)	d-1 (%)	d-2 (%)	Comments
Ni	110	S	c(2×2)	105	MEIS	ESA	H	100	2E + 20	L	—	1	1	298	—	—	—	1.246	0.87(03)(4F)	+ 6	—	Structure assumed for 0.5ML S. Bond length Ni–S 2.32A.
Ni	110	S	c(2×2)	93	LEIS	ICISS	Ne	5	6E + 18	—	LEED	3	3	—	—	—	—	1.246	0.89(0.05)	—	—	Possible substrate rearrangement.
Ni	111	—	(1×1)	106	HEIS	SB	He	500–2000	6E + 18	0.1%	MEED/AES	1	1	300	9	—	330	2.035	—	< 1	—	—
Ni	111	CO	(2×2)	107	LEIS	ESA	He	1.4	—	—	LEED/AES	4	4	—	—	—	—	2.035	—	—	—	CO associatively bonded through C atom: could not decide site. Same result for lower coverage ($\sqrt{7}/2\times\sqrt{7}/2$)R19.1 structure.
Ni	111	O	p(2×2)	108	HEIS	—	He	500–2000	—	L	LEED/AES	2	2	298	9,11	—	—	2.035	—	+ 7.4	—	Adsorbate-induced expansion also seen for ($\sqrt{3}\times\sqrt{3}$)R30 structure
Ni	111	O	p(2×2)	106	HEIS	—	He	500–2000	—	0.1%	MEED/AES	2	2	300	9	—	—	2.035	—	+ 7.3	—	—
Ni	111	S	(2×2)	93	LEIS	ICISS	Ne	5	6E + 18	—	LEED	3	3	—	—	—	—	2.035	1.61(0.06)	—	—	—
NiAl	110	—	(1×1)	109	MEIS	SB	H	100	—	L	LEED	2	2	—	53	RIS	220,320	2.04	—	− 7Ni, + 5Al	+ 1Ni, − 1Al	10% first layer ripple, Al on top.
$NiSi_2$	100	—	(1×1)	110	LEIS	LEIBAD	Li,He	5	3E + 19	L	LEED/AES	2	6+	—	111	—	—	1.351	—	− 22(4)	—	90Å film on Si(100). LEED I(V) curves agreed with [112]. Bulk-like Si termination; 25–30% vacancies.
Pb	110	—	(1×1)	113	HEIS	EAS/MC	H	50,97	—	L	LEED/AES	1	2	300	2,9	R2v	65	1.75	—	− 15.9(2.5)	+ 7.9	—
Pd	110	H	(1×2)	114	LEIS	ICISS/TOF	Ne	2	—	L	LEED	5	5	120	—	—	—	1.372	—	—	—	Row-pairing model preferred. Alternating lateral displacements of every other ⟨110⟩ row of about 0.4 Å with the same vertical shift.
Pd	111	—	(1×1)	115	HEIS	SB	He	1800	—	L	LEED/AES	3	5	300	—	—	—	2.240	—	0	—	No relaxation.
Pd	111	Au	(1×1)	115	HEIS	SB	He	1800	—	L	LEED/AES	3	5	300	—	—	—	2.240	—	—	—	Au grows pseudomorphically until 2 Å thick, then transition to strained misfit state.
Pt	100	H	(5×20)	116	HEIS	SB	He	1000–2000	?	L	LEED/NRA	2	4	120,297	118	—	239	1.961	—	0(0.5)	—	Reconstruction involves lateral diplace- of complete rows of atoms.
Pt	100	H_2CO	(5×20)	117	HEIS	SB	He	2000	?	L	LEED/XPS	2	4	175	118	—	115	1.961	—	< 1	—	Same result for both adsorbates.
Pt	110	—	(1×2)	119	LEIS	ICISS	Na	2	1E + 17	L	LEED/AES	7	7	—	—	—	—	1.387	—	—	—	Missing-row structure preferred, but some disorder.
Pt	111	—	(1×1)	121	HEIS	SB	He	400	—	< 0.1ML	LEED/AES	1	1	300	?	—	See Notes	2.264	—	< 2[av]	—	Used Debye temperatures of 115 K perpendicular and 235 K parallel.
Pt	111	—	(1×1)	122	HEIS	SB	He	2000	See Notes	< 0.1ML	—	3	6	40–300	123	—	200–400	2.264	—	+ 1.3(0.4)	—	Temperature-dependent damage responsible for earlier results showing large relaxation [124].
Pt	111	—	(1×1)	125	MEIS	ESA	H	173	—	< 0.1ML	—	1	1	—	—	—	< Bulk	2.264	—	+ 1.5(1.0)		
Pt	997	H	—	126	LEIS	LERS/TOF	Ne	10	—	L	—	1	2	220	—	—	174	—	0.7(0.2)(3F)	—	—	Also measured for Pt(445) surface. H occupies 3F hollow FCC site regardless of step orientation.
Si	100	(H)	(2×1)	127	HEIS	SB	He	100–2000	—	C/Si < 0.002	LEED/AES	1	Many	300	—	—	—	1.358	—	—	—	Compared with (1×1)-H termination. Evidence for subsurface strain with atomic displacements > 0.15 Å for at least 3 layers.
Si	100	—	(2×1)	41	LEIS	ICISS	He	1	—	L	LEED	2	2	—	—	—	—	1.358	—	—	—	Surface dimers; intradimer distance parallel to surface of 2.4(0.1) Å. Agrees with buckled dimer model [131].

TABLE 2. Surface structures determined by ion scattering (continued).

Subs.	Surf.	Ads.	Struct.	Ref.	Data Meth.	Data coll.	Ion	E(keV)	Dose (m^{-2})	Cont. level	Other tech.	Angs.	Data	Temp. (K)	Calcs.	R	Debye (K)	d-B (Å)	d-O (Å)	d-1 (%)	d-2 (%)	Comments
Si	100	—	(2×1)	128	MEIS	ESA	H	50–150	5E + 19	LC,O	LEED/AES	3	7	320	22	—	See Notes	1.358	—	—	—	Agreement best with buckled dimer model [131]. Parallel shifts of > 0.5 Å and subsurface distortions up to 3 layers deep. See also [129b].
Si	100	—	(2×1)	130	HEIS	TR/SB	He	1000,2000	—	L	MEED/AES	2	3	—	9	—	670(B)	1.358	—	—	—	YJM model [132] showed better agreement than symmetric [133] or buckled dimers [131] models.
Si	100	Au	—	134	HEIS	TC	He	2000	?	L	MEED/AES	1	Many	300	—	—	—	1.358	—	—	—	Si(100) film made by selective etching. Initial Au partially registered more random as approach 1 ML. Intermixing at 4 ML.
Si	100	H	(1×1) – 2H	129	MEIS	ESA	H	50–100	—	C/Si < 0.002	LEED/AES	2	5	323	11,22	—	230	1.358	—	– 6(3)	—	3000L H_2 with hot filament from (2×1) clean Si(100).
Si	100	Pd	(2×1)	159	MEIS	ESA	He	98,174	—	< 0.3%	LEED/EAS	1	1	—	—	—	—	1.358	—	—	—	Mixing occurs < 1 ML. Above 1 ML forms Pd_2Si. Si displaced at interface with silicide.
Si	111	—	(1×4)	141	MEIS	ESA	H	98	—	< 0.3%	LEED/AES	3	3	300	?	—	?	2.352	—	—	—	Laser annealed (7×7) surface. Results point to surface being disordered patches of (7×7).
Si	111	—	(2×1)	135	MEIS	—	H	99	—	—	—	1	1	—	—	R2v	—	2.352	—	See Notes	—	Tilted pi-bonded chains.
Si	111	—	(2×1)	136	MEIS	ESA/MC	H	99	—	L	LEED/AES	1	1	—	2	R2v	Several	2.352	—	See Notes	—	Cleaved in vacuum. Tilted pi-bonded chain model [137] best fit.
Si	111	—	(7×7)	137	HEIS	SB	He	100–4000	—	C/Si < 0.001	LEED/AES	2	Many	300	11	—	300–543	2.352	—	—	—	Major reconstruction involves vertical displacement of 0.4 Å. Lateral strain much smaller than Si(100) (2×1) < 0.15 Å. Surface vibrations enhanced by factor of 4.
Si	111	—	(7×7)	138	LEIS	ICISS	He	0.93	—	—	—	Many	Many	—	—	—	—	2.352	—	—	—	Densely-distributed pyramidal clusters of adatoms.
Si	111	—	(7×7)	142	MEIS	ESA/MC	H	99	—	—	—	1	1	—	9	—	—	2.352	—	See Notes	—	Data does not fit pyramidal cluster model. is consistent with stacking fault models [139,140].
Si	111	—	(7×7)	143	MEIS	ESA/MC	H	50–150	—	LC,O	LEED/AES	3	9	—	9,11	—	?	2.352	—	—	—	Data consistent with stacking fault models [139–140].
Si	111	Ag	(√3×√3)R30	144	LEIS	—	Ne	0.5	4E + 17	Trace C	LEED/AES	1	1	—	—	—	—	2.352	—	—	—	Ag atoms slightly embedded below top layer Si.
Si	111	Ag	(√3×√3)R30	145	LEIS	ESA	Ne	0.5	?	L	LEED/AES	—	—	300	—	—	—	2.352	—	—	—	Room-temperature deposition leads to island growth of commensurate Ag at 0.67 ML coverage. High-temperature (> 200 °C) deposition gives (√3×√3) structure with Ag embedded in first Si layer.
Si	111	Ag	(√3×√3)R30	148	LEIS	ICISS	Li	1	—	—	—	5	Many	—	—	—	—	2.352	—	—	—	Honeycomb structure above Si layer.
Si	111	Ag	(1×1)	147	MEIS	ESA	He	175	—	C,O < 0.3%	LEED/AES	1	4	300	—	—	—	2.352	—	—	—	Deposited on (7×7) surface to give 2 then 3-D growth. No intermixing, 2 domains.
Si	111	Ag	—	146	HEIS	SB	He	1000	?	< 0.2%C	MEED/AES	1	Many	300	12	—	—	2.352	—	—	—	Amorphous film on (7×7) surface. No mixing < 1 ML, for > 3 ML silicide formed.
Si	111	Al	—	149	HEIS	—	He	800–2000	—	—	—	1	Many	300	—	—	—	2.352	—	—	—	Al deposited from ionized cluster beam. Al(111) grows epitaxial despite large lattice mismatch
Si	111	Au	(√3×√3)R30	150	LEIS	ICISS	Na	0.9	—	L	LEED/AES	2	2	300	—	—	—	2.352	0.3	—	—	Deposition at 700 °C, coverage = 1 ML. Au triplet clusters on Si honeycomb structure.
Si	111	Au	(5×1)	151	LEIS	—	Ne	0.5	2E + 16	C/Si = 1/800	LEED/AES	1	1	300	—	—	—	2.352	—	—	—	Deposited at 700 °C, coverage 0.4 ML. Au atoms embedded below outermost Si layer (3 domains).
Si	111	Au	—	146	HEIS	SB	He	1000	?	C < 0.2%	LEED/AES	1	Many	300	12	—	—	2.352	—	—	—	Amorphous film on (7×7) surface. No mixing < 1 ML, for > 3 ML silicides form.

TABLE 2. Surface structures determined by ion scattering. (continued).

Subs.	Surf.	Ads.	Struct.	Ref.	Data Meth.	Data coll.	Ion	E(keV)	Dose (m^{-2})	Cont level	Other tech.	Angs.	Data	Temp. (K)	Calcs.	R	Debye (K)	d-B (Å)	d-O (Å)	d-1 (%)	d-2 (%)	Comments
Si	111	Br	$(\sqrt{3}\times\sqrt{3})R30$	152	HEIS	TC/SB	He	2500	L	L	AES	2	2	—	—	—	—	2.352	0.875(1F)	—	—	Br adsorbed to thinned crystal from solution *ex situ*. Assumed bulk-like substrate.
Si	111	Ge	—	155	HEIS	SB	He	1000	?	L	LEED/AES	1	Many	300	12	—	—	2.352	—	—	—	Deposited on (7×7) surface at 300–600 °C. At room temperature, amorphous film; at 350 °C, epitaxial growth occurs up to 1 ML; above this strained structure. Above 450 °C intermixing.
Si	111	Ni	—	156	HEIS	SB/TC	He	1000	—	C<0.1%	LEED/AES	1	Many	170,300	—	—	—	2.352	—	—	—	—
Si	111	$NiSi_2$	(1×1)	157	MEIS	ESA	H	100	—	L	LEED/AES	1	Many	300	233	—	—	2.352	—	—	—	Ni deposited on (7×7) surface and heating to 770 K/5 min, to give 25Å-thick $NiSi_2$ film. Ni atoms at interface are 7-fold coordinate and bonds at the interface are relaxed.
Si	111	Pd	$(\sqrt{3}\times\sqrt{3})R30$	158	LEIS	—	Ne	0.5	—	L	LEED/AES	1	1	300	—	—	—	2352	—	—	—	0.5 ML Pd atoms lie below top layer of Si atoms.
Si	111	Pd	—	146	HEIS	SB	He	1000	?	C<0.2%	MEED/AES	1	Many	300	12	—	—	2.352	—	—	—	Deposited on (7×7) surface to form silicides at all coverages.
Si	111	Pd	—	159	MEIS	ESA	He	98,174	—	C,O<0.3%	LEED/AES	1	1	—	—	—	—	2.352	—	—	—	For <1 ML 2-D growth, no mixing. Above 1 ML Pd_2Si formation. Attribute differences with [146] to damage.
Si	111	Ti	—	160	MEIS	ESA	He	175	—	C,O<0.4%	LEED/AES	1	Many	300	—	—	—	2.352	—	—	—	Ti deposited on (7×7) surface. Mixing occurs at room temperature to give TiSi, with may displaced Si atoms at interface.
TiC	001	O	(1×1)	161	LEIS	—	He	1	—	O<1%	LEED/AES	3	3	300	—	—	—	—	—	—	—	O adsorbed on C atoms.
UO_2	100	—	c(2×2)	162	LEIS	CMA	He	0.5	?	L	LEED/AES	2	2	873	—	—	—	—	—	—	—	Monolayer of O atoms in distorted bridge-bonded zig-zag chains along ⟨100⟩.
UO_2	110	—	—	163	LEIS	CMA	He	0.5	?	—	LEED/AES	2	2	<773	—	—	—	—	—	—	—	Facets above 600 °C. U and O coplanar.
UO_2	111	—	—	164	LEIS	CMA	He	0.5	?	L	LEED/AES	2	2	873	—	—	—	—	—	—	—	Outermost layer is O occupying bulk-like positions.
UO_2	553	—	—	164	LEIS	CMA	He	0.5	?	L	LEED/AES	2	2	873	—	—	—	—	—	—	—	Ledge U is covered with excess O.
W	100	—	(1×1)	165	HEIS	SB	He	2000	—	L C,O	LEED/AES	3	3	300	11	—	384(B)	1.578	—	< −6	—	Signs of disorder at room temperature.
W	100	H	c(2×2)	166	HEIS	SB	He	600–2000	6E + 18	—	LEED	2	6	300	9	—	—	1.578	—	—	—	Data not consistent with buckling [234] or zig-zag chains [179b].
W	211	D_2	—	167	LEIS	CMA	He	0.3	?	L	LEED/AES	2	2	300	—	—	—	1.37	—	—	—	Beta-2 D_2 thermal desorption state located in deep trough positions.

2F(S) = 2-fold coordinate short-bridge site, e.g., FCC(110)

2F(L) = 2-fold coordinate long-bridge site, e.g., FCC(110).

1F = 1-fold coordinate site directly on top of another atom

d-1:

The value of the vertical interlayer spacing between the 1st and 2nd layer of the solid expressed in terms of a percentage change from the bulk value. Error in parentheses when given.

d-2:

The value of the vertical interlayer spacing between the 2nd and 3rd layer of the solid expressed in terms of a percentage change from the bulk value. Error in parentheses when given.

The entries used in Table 2 obey the following restrictions:

(1) Articles published in unrefereed conference proceedings or society bulletins were not used.

(2) Papers on thin films and buried interfaces that did not explicitly consider surface structures were not considered.

(3) A series of investigations by the same principal author on the same topic are grouped into one table entry using the latest set of data/results, but all references are provided.

5. Discussion of Structural Results

5.1. Clean Metal Surfaces

Clean metal surfaces were the earliest types of system to be studied by surface crystallographers and interest persists to the present day. Most studies have focussed on the low-index faces of the face-centered cubic (FCC) metals. The body-centered cubic (BCC) materials W, Fe, and Mo have also received attention, while as yet the hexagonal close-packed metals have not been studied by ion crystallography. For reference, Figure 1 shows the arrangement of surface atoms for some ideal low-index metallic planes.

In the following sections we discuss the surface crystallographic results from ion scattering and LEED. Many metal surfaces closely resemble a truncated bulk lattice, but an increasing number of systems are revealing multilayer oscillatory relaxations. Some surfaces, in particular the (100) and (110) surfaces of Ir, Pt, and Au, exhibit reconstructions that can involve vertical and lateral displacements of atoms from their bulk positions.

5.1.a. Almost Ideal Surfaces

Early LEED studies have shown that, with only a few exceptions, many of the high-density low-Miller-index surfaces of metals do not reconstruct or alter their topmost interlayer spacing (d_1) by more than a few percent ($< 5\%$) of the bulk value (d_B), usually in the form of a contraction. The ion scattering studies of these surfaces have been gathered together in Table 3 with corresponding LEED studies,[1] where available. In general the agreement between ion scattering and LEED results is good, as good as the internal agreement within either technique on its own.

The Pt(111) and W(100) surfaces provide interesting case histories. Some of the very first channeling studies surfaces were carried out on Pt(111). The initial result of 15% expansion by HEIS[124] was in strong disagreement wi LEED[171–173] data that showed little or no expansion or co traction. Later HEIS[121,122] and MEIS[125] studies agreed wi the LEED results. The initial contradiction was likely due beam damage or contamination.

The W(100) (1×1) surface has received a high degr of attention from LEED workers with a variety of resul which eventually have settled down to a value close -7% for d_1. The HEIS study by Feldman *et al.*[165] on tl surface gave a very similar result of a contraction of up 6.7%.

The Pt(100) surface in its clean state is reconstruct (see below); a HEIS study,[116] which has not been duplicat using LEED, of a H-stabilized surface showed a nearly id bulk termination.

5.1.b. Multilayer Relaxed Surfaces

One of the most interesting surface structural results have been discovered recently has been the occurrence multilayer oscillatory relaxations of surfaces such FCC(110), and others with low packing densities. Here take *relaxation* to mean changes in the perpendicular int layer spacings relative to the bulk value, whereas *reconstr tions* involve lateral shifts in atomic position. Several met have been found to exhibit damped oscillatory variations their interlayer spacings, extending sometimes up to 4 lay into the interior of the crystal. Such investigations requir careful approach in order to detect such small structu changes.

A summary of results for such surfaces can be found Table 4. The Ni(110) surface has been extensively studi and has provided some difficulties. This surface was exa ined early in the history of the MEIS technique and found be bulk-like,[94] or to have a slightly contracted d_1 (-4% Later MEIS experiments by Tornqvist *et al.*[97] confirmed t result, and Feidenhans'l *et al.*,[96] using HEIS, showed e dence for an expansion of d_2 ($+2.4\%$).

Corresponding LEED studies have also had their d culties. Early work favored contractions of d_1 close to 5 but later investigations produced values of -9% for d_1 a $+3\%$ for d_2.[184–186]

A further MEIS report from Yalisove *et al.*[98] found c tractions of d_1 in agreement with the LEED results. T authors attribute the discrepancy with earlier experiment contamination problems. We can note that the use of blc ing in MEIS studies gives higher sensitivity to multila relaxations than do HEIS rocking curves. Blocking m surements around the appropriate exit direction dire yield the change in d_1; further measurements in directi which probe deeper into the crystal then give informatio d_2. On the other hand, HEIS rocking curves are rather sensitive to multilayer effects, as opposing contraction expansions in the first two layers can reduce the asymm of the rocking curve until it resembles that from an u laxed surface.

The Cu(110) surface provides another example of level of agreement between ion scattering and LEED stuc

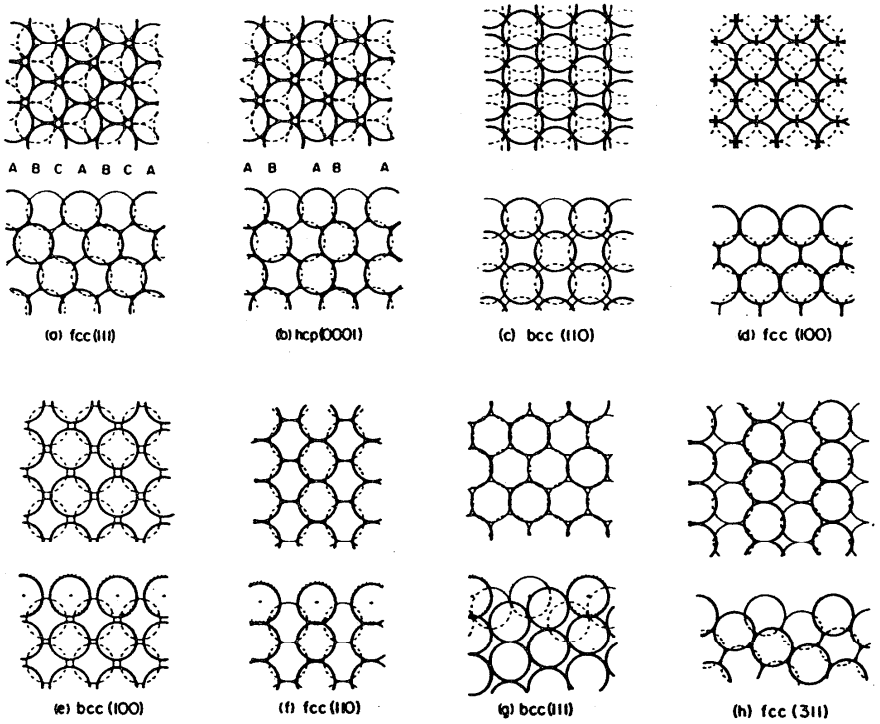

FIG. 1. Schematic diagram of the ideal structures of some simple low-index surfaces of metals. In each panel the top and bottom parts are top and side views, respectively. Thin-lined atoms lie behind the plane of thick-lined atoms; dotted lines represent atoms in bulk positions (Ref. 229).

ɔle 3. Structural parameters[a] derived for nearly ideal metal surfaces studied by ion scattering compared with LEED[1].

ɪrface	Bulk d_B (Å)	δd_1 (%)	Method	Ref.
ɜ(100)	1.433	0.0	LEIS	78
		-1.4	LEED	231
i(100)	1.762	-3.2	MEIS	82
		0.0	LEED	168
		0.0 ± 4.0	LEED	169
		0.0 ± 2.5	LEED	170
i(111)	2.035	< |1|	HEIS	106
		0.0	LEED	169
		0.0	LEED	170
ɨ(111)	2.228	0.0	HEIS	115
		0.0	LEED	232
ɜ(100)[b]	1.981	0.0	HEIS	116
ɜ(111)	1.732	-15	HEIS	124
		< |2|	HEIS	121
		+1.3 ± 0.4	HEIS	122
		+1.5 ± 1.0	MEIS	125
		0.0 ± 5.0	LEED	171
		0.0 ± 2.5	LEED	172
		+1.0 ± 0.5	LEED	173
(100)[c]	1.578	<-6.7	HEIS	165
		-6.0 ± 1.0	LEED	174
		-11.0 ± 2.0	LEED	175
		-5.5 ± 1.5	LEED	176
		-10.0 ± 2.0	LEED	177
		-6.7 ± 1.0	LEED	178
		-8.0 ± 1.5	LEED	179
		-7.0 ± 1.5	LEED	180

ɔxpressed as percentage change from the bulk value

ɜtabilized with H_2

1x1) phase

HEIS work by Stensgaard *et al.*[66a] and the studies of Copel *et al.*[69] favor a first layer contraction of ~6%, and a second layer expansion of ~2 to 3%. These contrast with the LEIS work of Yarmoff *et al.*,[67] which produced a value for d_1 of −10%. LEED studies by Davis *et al*[183] showed a rather larger value for d_1 of −9% and agreed with d_2. The HEIS results and further LEED data of Adams and coworkers,[182] showing a similar larger value for d_1 of −8.5%, were later reconciled.[66b]

We might also note that in Table 4 there are two ion scattering studies with no LEED counterparts. Strictly speaking, as the Mo(111) investigation[88] only explored variations in d_1, we should not include it as an example of multilayer effects. The size of the contraction found (18%) is large enough to make one suspect their presence; however, it should be borne in mind that d_B for Mo(111) is a relatively small 0.90 Å, and hence a large percentage change is not so large in absolute magnitude. Frenken *et al.*[113] also found for Pb(110) an unequivocally large multilayer effect using MEIS; this would be an interesting surface for LEED studies.

5.1.c. High-Index Surfaces

High-index surfaces offer more possibilities for the relaxation of atoms away from their bulk positions. A number of such surfaces have been studied by LEED crystallography,[1] revealing a variety of perpendicular and parallel movements of atoms that still preserve the (1×1) surface symmetry. Studies of such surfaces using ion scattering are just

Table 4. Structural parameters[a] derived for metal surfaces exhibiting multilayer relaxations by ion scattering compared with LEED[1].

Surface	Bulk d_B (Å)	δd_1 (%)	δd_2 (%)	δd_3 (%)	Method	Ref.
Ag(110)	1.445	-7.8 ± 2.5	+4.3 ± 2.5	--	HEIS	17
		-9.5 ± 2.0	+6.0 ± 2.5	--	MEIS	25
		-5.7 ± 2.0	+2.2 ± 2.0	--	LEED	181
Cu(110)	1.278	-5.3	+3.3	--	HEIS	66
		-10 ± 5	--	--	LEIS	67
		-7.5 ± 1.5	+2.5 ± 1.5	--	MEIS	69
		-8.5 ± 0.6	+2.3 ± 0.8	-0.9 ± 0.9	LEED	182
		-9.1	+2.3	--	LEED	183
Mo(111)	0.907	-18 ± 2	--	--	LEIS	88
Ni(110)	1.246	0	--	--	MEIS	94
		-4 ± 1	--	--	MEIS	95
		-4.8 ± 1.7	+2.4 ± 1.2	--	HEIS	96
		-4 ± 1	--	--	MEIS	97
		-9.0 ± 1.0	+3.5 ± 1.5	--	MEIS	98
		-8.7 ± 0.5	+3.0 ± 0.9	-0.5 ± 0.7	LEED	184
		-8.4 ± 0.8	+3.1 ± 1.0	--	LEED	185
		-9.8 ± 1.8	+3.8 ± 1.8	--	LEED	186
Pb(110)	1.750	-15.9 ± 2.5	+7.9 ± 2.5	--	MEIS	113

[a] expressed as percentage change from the bulk value d_B

starting to appear in the literature e.g. Cu(410),[74] Cu(16,1,1),[76] Pt(997).[126]

5.1.d. Reconstructed Surfaces

The (110) surfaces of Au, Ir, and Pt exhibit a (1×2) reconstruction when clean. The Au surface in particular has been the subject of numerous ion scattering and LEED investigations. A number of possible surface structures have been proposed involving hexagonal close-packed overlayers, paired rows, buckled, and missing rows. In general the consensus appears to favor a structure with a missing row of atoms in the [— 110] direction in the surface leading to a doubling of the unit cell in the [001] direction as shown in Fig. 2. The Au surface structure seems to be the best established with a large contraction of the 1st layer, a small lateral pairing displacement of the 2nd layer and a possible buckling of the 3rd layer. The existence of the missing row does not seem to be in doubt, it having been also seen by electron microscopy,[190] and the scanning tunneling microscope.[191] However, some differences in detail exist between MEIS,[56,60] HEIS,[16] and LEED[187] results (See Table 5).

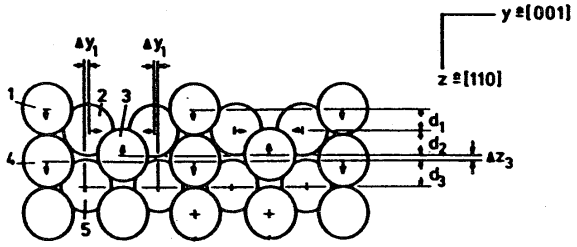

FIG. 2. Schematic diagram of the missing-row model of the (2×1) reconstructed (110) surfaces of Au, Ir, Pd and Pt.[187]

LEED studies of Ir(110)[188] found the missing r model with a large contraction of the 1st layer spacing, sir lar to that in Au(110), to produce a slightly better fit tha row-pairing or buckled-surface model. The correspondi MEIS study,[60] on an apparently only partially reconstruct surface, was in agreement with the overall structure.

The position for Pt(110) is less clear. A LEED study and LEIS [119] work again tended to favor a missing-row rangement, while an HEIS investigation by Jackman *et al.* concluded that their data excluded any significant late displacements or vertical shifts. Rocking scans both norn and off-normal to the surface were extremely symmetri implying that any lateral movement from bulk positions h to be <0.02 Å, and vertical shifts of <0.07 Å. This d suggests that the Pt(110) and Au(110) reconstructions possibly rather different; the HEIS data is consistent with unrelaxed, or very weakly buckled, surface.

The normal (1×1) W(100) surface undergoes a tr sition to a reconstructed c(2×2) form below 300 K, or exposure to hydrogen. Two HEIS studies[165,166] agree w LEED data[192,193] in finding a small contraction in d_1. T LEED structure of Debe and King[179] has atoms in the [1 direction forming a zig-zag row structure as shown in Fig The ion scattering results of Stensgaard *et al.*[166] indicate t about one-half of a monolayer of atoms have shifted p tion. This is consistent with the zig-zag chain model if rec structed domains coexist with bulk-like areas that are sta lized by some surface defect.

5.2. Adsorbate-Covered Metal Surfaces

The variety of adsorbate systems that have been stud by ion scattering is rather small. Most investigations h involved O or S chemisorption, most usually on Cu and

Table 5. Structural parameters from ion scattering and LEED for the missing-row structure for the (1x2) reconstructed (110) surfaces of Au, Ir and Pt[a].

	d_B (Å)	d_1 (Å)	d_2 (Å)	d_3 (Å)	δz_3 (Å)	δy_1 (Å)	Method	Ref.
Au(110)	1.442	1.19	--	--	--	<0.1	LEIS	59
		1.18	1.49	--	0.10	<0.1	MEIS	56,60
		1.19	--	--	--	0.18	HEIS	16
		1.15	1.35	1.35	0.23	0.07	LEED	187
Ir(110)	1.352	1.23[b]	--	--	--	--	MEIS	60
		1.16	1.16	--	<0.2	<0.2	LEED	188a
		1.19[c]	1.20	1.28	0.23	0.10	LEED	188b
Pt(110)[d]	1.387	1.39	--	--	<0.02	<0.07	HEIS	120
		1.7	1.38	--	--	0.05	LEED	189

[a] parameters are defined in Figure 2.

[b] surface apparently not homogeneous

[c] paired rows in second layer, and buckled rows in third layer

[d] data consistent with very weakly buckled surface

ecause of their small cross sections for scattering, adsorbates such as C and O are difficult to detect by shadowing and blocking. However, the changes in blocking patterns are often sufficient to establish the location of the adsorption site, and the height of the adatom above the surface d_0.

There appears to have been only one true case of molecular adsorption studied, that of CO/Ni(111).[107] This experiment showed the CO bonded through the C atom as has been found in many other metal/CO systems by LEED.[1]

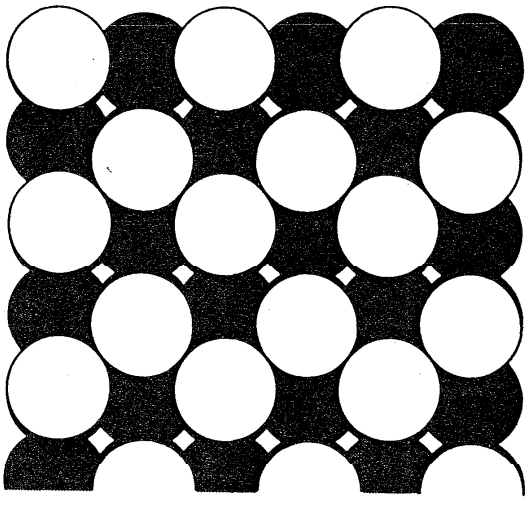

FIG. 3. Schematic diagram of the W(100) c(2×2) reconstructed surface structure (Ref. 230).

5.2.a. Simple Atomic Adsorption

In the main, atomic species adsorbed on low-index surfaces have been found to occupy the high-symmetry sites shown in Fig. 4. Sometimes adsorption is accompanied by rearrangements of the substrate as discussed below, but often the chemisorption appears to be simple. This simplicity may be more apparent than real as many LEED and ion scattering studies have assumed that chemisorption did not induce reconstruction.

The adsorption sites are described in Table 2 as XF, meaning X-fold coordinate, considering only the 1st shell of nearest neighbors. In some cases, alternate sites of the same coordination are distinguished by the arrangement of metal atoms making up the site, e.g., 2F(S) and 2F(L)-short and long 2-F bridge sites on an FCC(110) surface.

Table 6 summarizes the ion scattering and LEED results for these systems. There is almost perfect agreement between the two techniques on adsorption sites, and d_0 values agree within a small margin. The Cu(100)–O system has presented difficulties and probably involves penetration of O atoms into the surface, particularly at higher coverages.

5.2.b. Adsorption-Induced Surface Reconstruction

Changes in the geometry of substrate atoms due to adsorption fall into two classes: alteration, usually removal, of a reconstruction or relaxation pre-existing on the clean surface, or the formation of a new reconstruction of the metal atoms.

The removal of a clean surface reconstruction upon adsorption has been followed in a few cases by ion scattering. The best examples involve platinum. The conversion of the (1×2) Pt(110) and the Pt(100) (5×20), or "hex", recon-

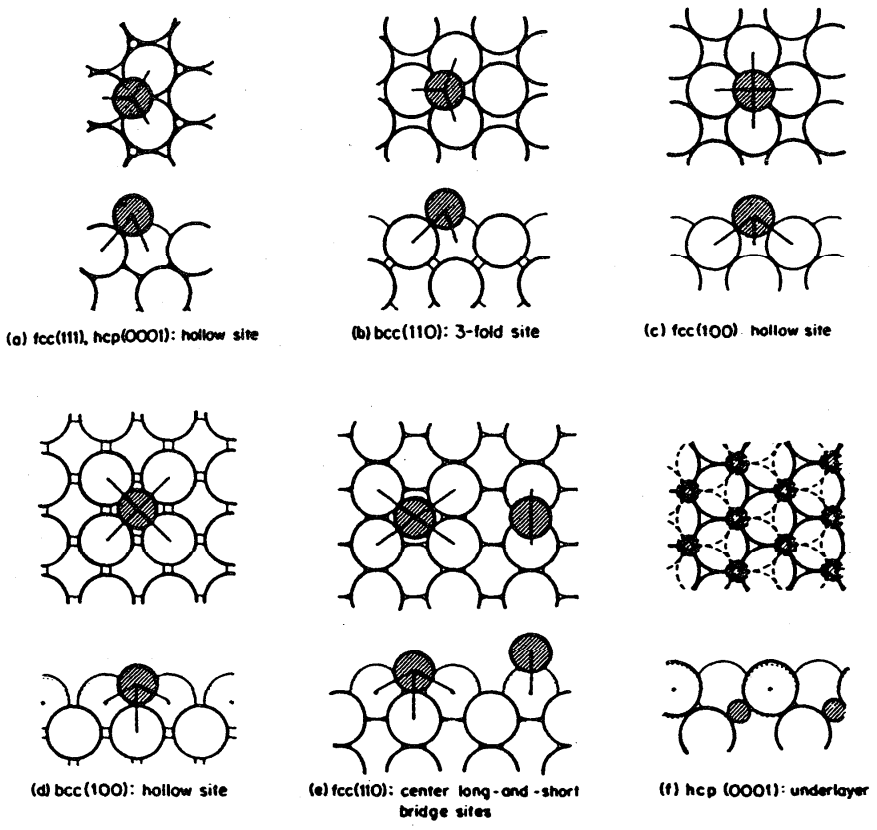

FIG. 4. Schematic diagram (top and side views) of high-symmetry adsorption sites on low-index surfaces of metals (Ref. 229).

Table 6. Adsorption sites and distances for systems showing no reconstruction due to adsorption determined by ion scattering and LEED.

Surface	Adsorbate	Structure	Site	d_0(Å)	Method (Å)	Ref.
Ag(110)	O	(2x1)	2F-L	0.0	LEIS	48
				--	LEED	194
Cu(100)	O	c(2x2)	2F/4F	--	LEIS	32,64
			2F?	1.4	LEED	195
Fe(100)	O	(1x1)	4F	0.56	LEIS	79
			4F	0.48	LEED[a]	196
Ni(100)	D	--	4F	0.5	HEIS	90a,b
	O	c(2x2)	4F	0.90	LEIS	92
				0.86	MEIS	89
				0.90	LEED	197, 198
				0.80	LEED	199
	S	c(2x2)	--	1.40	LEIS	93
				1.30	LEED	200-202
Ni(110)	S	c(2x2)	4F	0.87	MEIS	105
				0.89	LEIS[b]	93
				0.84	LEED	203
Ni(111)	CO	(2x2)	--[c]	--	LEIS	107

[a] also found $d_1 = -7.5\%$

[b] probable reconstruction

[c] adsorbed through C atom

structions to (1×1) by hydrogen or CO were studied by the Chalk River group.[116,120]

Many metals show significant changes in the degree of relaxation of their surface layers on adsorption by ion scattering and LEED. They are summarized in Table 7.

The most interesting feature of Table 7 is that expansion of the surface upon adsorption of 0.5 monolayers of O or S appears to be common. On clean surfaces that are contracted, the expansion induced by adsorption can be great enough to result in an overall expansion of d_1. Thus the MEIS experiments of van der Veen *et al.*[105] showed that the 8% contraction of clean Ni(110) turned into a 5% expansion with 0.5 monolayers of adsorbed sulfur.

Adsorbate-induced reconstructions of the underlying substrate atoms are becoming a feature of surface crystallography. Two prominent cases that have been extensively investigated by the ion scattering community are the (2×1) O-induced reconstructions of Cu and Ni(110).

The Ni(110) (2×1) reconstruction has generated a significant amount of discussion. Early LEIS work by Verheij *et al.*[100] indicated the presence of a reconstruction and identified the adsorption site as a long-bridge site. Later MEIS shadowing/blocking studies by Smeenk *et al.*[101] gave strong evidence for a missing-row reconstruction. This has been further supported by ICISS work by Niehus and Comsa,[103] while Schuster and Varelas[102] have suggested a saw-tooth modification.

For Cu(110), LEIS results[67,70] suggest a missing-row structure, while HEIS studies[71] prefer a buckled-row model. It may well be that the differences between investigations will boil down to the fact that the exact condition of the surface in the case of these adsorbate-induced reconstructions depends critically upon the method of preparation. There is evidence that the temperature of exposure may be a crucial variable.[2]

5.3. Semiconductor Surfaces

5.3.a. Silicon Surfaces

The cleaved Si(100) surface exhibits a (2×1) LEED pattern indicative of a reconstruction. Adsorption of hydrogen results in a (1×1) pattern that has been shown to be due to an essentially truncated bulk structure by both MEIS[127,129] and LEED.[204]

The (2×1) reconstruction has been the subject of a number of studies. Models for the surface geometry have basically revolved around two concepts—either surface vacancies, or dimerization of surface atoms, similar to the paired-row and missing-row models for Au(110). A number of these models are shown in Figure 5.

An ICISS study by Aono[41] found evidence for surface dimers; in addition LEED[205] and STM[206] evidence also pointed to surface dimerization as being the correct model. A MEIS study by Tromp *et al.*[128] found that models involving symmetric dimers did not fit their data. Blocking patterns taken in various scattering geometries were in agreement with a buckled or asymmetric dimers,[131] in which one of the paired atoms sinks deeper into the surface than the other, and also included subsurface distortions. This model has the added attraction that the occasional finding of c(4×2) LEED patterns can be explained by suitable arrangements of these buckled dimers.

The most recent LEED[207,208] experiments and the transmission HEIS work of Jin *et al.*[130] confirm this general picture, but find that a twisting of the asymmetrical dimer around an axis perpendicular to the surface improves the agreement with experiment. This model is shown in Fig. 6, and crystallographic data collected in Table 8. Unfortunately, total energy calculations[128,209] for the Yang *et al.* model[208] indicate that displacements perpendicular to the (110) plane are destabilizing. Hence, although the major features of the Si(100) (2×1) surface appear to be under control, the fine details are in doubt.

The (111) surface of Si has been one of the most studied of all surfaces in surface science, and it has received due attention from the practitioners of ion scattering. The vacuum cleaved surface shows a (2×1) LEED pattern that evolves to a (7×7) structure after annealing. The surface relaxes to a (1×1) structure if laser annealed, or quenched at high temperatures. It can also be stabilized by small amounts of impurities such as Te.

Many models involving buckling,[210,211] molecular[212] and pi-bonded chains,[213] and conjugated chains[214] have been proposed to account for the (2×1) LEED pattern observed

Table 7. Relaxations of metal first interlayer spacings upon adsorption[a], determined by ion scattering and LEED.

Metal	δd_1 (%) clean surface	Adsorbate	δd_1 (%) after adsorption	Method	Ref.
Ni(100)	0	c(2X2)-O	+5.2	MEIS	89
Ni(110)	-8.4	c(2X2)-S	+6 +10	MEIS LEED	105 203
Ni(111)	0	(2x2)-O	+7.4	HEIS	106 108
Pt(111)	0	(1x1)-CO	+0.8	HEIS	120

[a] Expressed as percentage changes from the bulk value d_B.

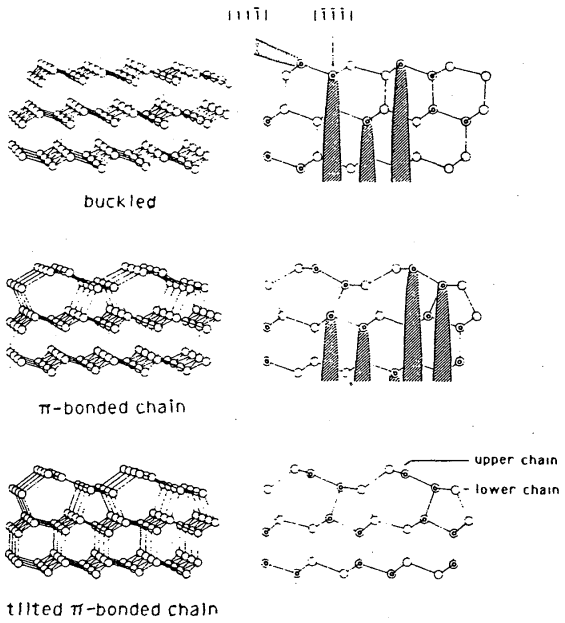

FIG. 5. Different models proposed for the Si(100) (2×2) reconstruction. (Ref. 2).

Table 8. Atomic geometry of buckled dimer models of t Si(100) (2X1) surface[a].

	Yin and Cohen[104]			Yang et al[208]		
Atom	δx	δy	δz	δx	δy	δz
Si_{11}	-0.520	0	0.160	-0.650	-0.300	0.04
Si_{12}	1.040	0	0.468	0.750	0.300	0.44
Si_{21}	-0.094	0	0.047	-0.060	-0.100	0.13
Si_{22}	0.115	0	-0.020	0.120	0.100	0.13
Si_{31}	0	0	-0.139	0	0	-0.15
Si_{32}	0	0	0.185	0	0	0.20

[a]Parameters are defined in Figure 6.

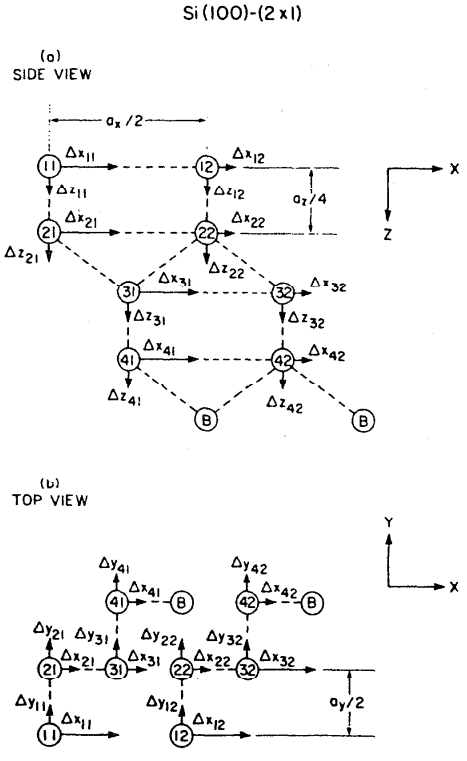

FIG. 6. Schematic diagram of the asymmetric dimer geometry of the (2×1) structure of Si(100) (Ref. 207). (a) Projection of the 2×1 unit cell on {110} plane of bulk Si ($a_x = 7.68$ Å, $a_y = 5.44$ Å). (b) Projection of the 2×1 unit cell on the {001} plane of bulk Si ($a_y = 3.84$ Å).

from cleaved Si(111). Two MEIS studies[135,136] agree w the most recent LEED study[214] in favoring a modified bonded chain model in which the outer chain is buckled w an overall compression. This structure is detailed in Fi and Table 9.

The (7×7) reconstruction of Si(111) has been a m challenge to surface scientists. Ion scattering studies[137] have played a significant role in unravelling this structure fact this surface has shown the value of combining the in mation available from many different surface science te niques.

Because of the size of the (7×7) unit cell, early k matic LEED studies on this surface produced a large n ber of competing models for the structure (see Ref. 216 Refs. therein). The first HEIS experiments by Culbertso *al.*[137] required unreasonably large perpendicular displ ments of up to 0.5 Å for the atoms in the first two layers. T data was reanalyzed by Bennett *et al.*[140] in terms of a st ing fault dividing the surface up into triangular areas. T idea was enlarged upon by Himpsel and Batra[215] McRae,[139] who noted that the topological requirement joining double layers at the subunit boundaries should l to arrays of dimers and deep holes. Further MEIS exp ments by Tromp and van Loenen[142,143] support the stack fault model and showed that the LEIS results of Aon *al.*[138] could be interpreted in these terms.

The situation was clarified by the transmission elect diffraction experiments of Takayanagi *et al.*,[217] and the r space images provided by Binnig *et al.*[218] using the scan tunneling microscope. These results, coupled with the lier ion scattering and LEED data were reconciled in dimer-adatom-stacking fault (DAS) model shown in Fi In this model, the outermost double layer consists of triangular subunits which are, respectively, faulted and faulted with respect to the substrate. The partial dislocat at the border of the triangular subunits are reconstru into 12-membered rings surrounding a corner hole 6.

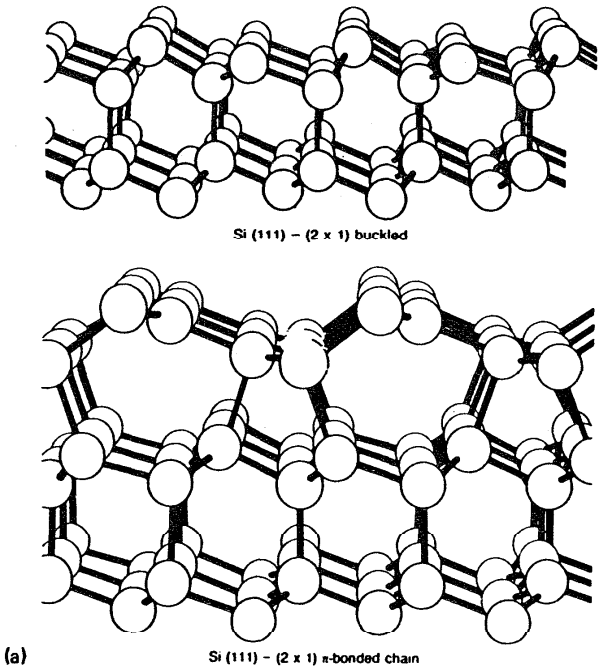

FIG. 7. (a) The buckled and pi-bonded chain models for the Si(111) (2×1) reconstruction (Ref. 230). (b) Schematic diagram of the buckled pi-bonded chain model for the (2×1) structure of Si(111) showing a side view (Ref. 214).

deep, together with alternating dimers and 8-membered rings.

The DAS model has come to be generally accepted as containing all the correct ingredients of the (7×7) structure, but some important information remained missing, e.g., vertical distances between atoms. Employing a new theoretical approach, Tong *et al.*[220] have performed a full LEED analysis on this structure and produced a refined version of the DAS model. This model, which contains the coordinates for 200 atoms in the first five atomic layers, shows an oscillatory relaxation with atomic planes having stretched bonds followed by ones in which the bonds are compressed.

The Si(111) (7×7) reconstruction can be quenched to (1×1) by the presence of impurities, or laser annealing. Tromp *et al.*[141] found by MEIS that the laser annealed (1×1) surface shared many of the basic structural features of the (7×7) reconstruction, possibly consisting of disordered areas of the reconstructed material. This result contradicted an earlier LEED study of Zehner *et al.*[221] that favored a bulk-like surface with a contracted first layer spacing. A later LEED study, however, found as good agreement with a graphitic top double layer of Si atoms.[222]

5.3.b. Si/adsorbate Systems

Studies of adsorbed gas phase species on Si by ion scattering are relatively rare. H and D adsorption on Si(100)[127,129] and (111)[154] have been valuable in understanding the reconstructions of these surfaces. There is also an interesting transmission HEIS study by Gibson and coworkers[152] of bromine adsorbed from a bromine/ethanol solution onto Si(111), which found the halogen to be bound directly over the first layer Si atoms.

Much of the recent work in channelling has been directed towards understanding the growth of metallic thin films on Si surfaces, particularly those used in electronic device manufacture. Important goals are to characterize the growth mode, defect formation, and the nature of buried interfaces. Such studies are in general not included here, but there are a number of investigations in this area that have defined the early stages of growth and provided surface structural results.

The largest number of ion scattering studies concern the growth of the noble metals Ag and Au on Si(111) and (100); there are few LEED counterparts. Both HEIS,[134,136] MEIS,[147] and LEIS[144,145,148,150,151] have shown little intermixing of the elements at room temperature for coverages up to a monolayer. Silicide formation occurs at higher coverages.[134,146] Heating a Si(111) (7×7) surface that contains a monolayer or so of Ag results in a $(\sqrt{3}\times\sqrt{3})$R30° structure that has been studied by two different groups using LEIS, with differing conclusions. Saitoh *et al.* concluded, from ICISS[144,145] and LEED,[223] that Ag atoms were slightly embedded below the topmost Si layer [Figure 9(a)]. Aono and coworkers[146] interpreted their ICISS data as a honeycomb arrangement of Ag atoms located above the first Si layer [Figure 9(b)]; Oura *et al.*[150] have proposed a similar structure for the analogous Au $(\sqrt{3}\times\sqrt{3})$R30° system.

The interaction of Pd with Si surfaces appears to be qualitatively different in that spontaneous formation of a mixed Pd–Si layer occurs with the composition Pd_2Si.[149,159] For Ti, MEIS measurements show that the mixing occurs at room temperature to give TiSi, which then becomes coated with a pure Ti layer upon further adsorption.[160]

Table 9. Atomic geometry for the buckled pi-bonded chain model of Si(111) (2x1) structure[a].

Atom	X	Y	Z
1	1.09	1.92	-3.90
2	4.45	0.0	-3.93
3	2.21	0.0	-3.21
4	5.54	1.92	-3.08
5	2.22	0.0	-0.89
6	5.54	1.92	-0.69
7	0.09	0.0	-0.02
8	3.24	1.92	-0.09
9	0.95	0.0	2.18
10	2.34	1.92	2.11
11	4.34	1.92	3.37
12	5.46	0.0	2.99

[a]The x,y,z coordinates (Å) refer to the [-12-1], [-101], and [111] directions shown in Figure 7 with the origin at a third layer atom of the truncated bulk lattice[214].

5.3.c. III-V Semiconductors

The cleavage (110) surface of III-V semiconductors is nonpolar and retains the (1×1) surface unit mesh expected for a truncated bulk structure. However, it was soon discovered that GaAs(110) is in fact reconstructed in a subtle manner. The solution of this structure became something a cause célèbre in the LEED community.

Initial LEED work suggested two models where t surface is relaxed from its bulk configuration through bo rotations (ω in Fig. 10 in the first bilayer.) In the bor rotation model[224] a rotation of $\sim27°$ allowed for conser tion of bond lengths. The alternative bond-relaxation mo needs a much smaller rotation angle of 7°.[225] Further LEI work favored the bond-rotation structure.[226]

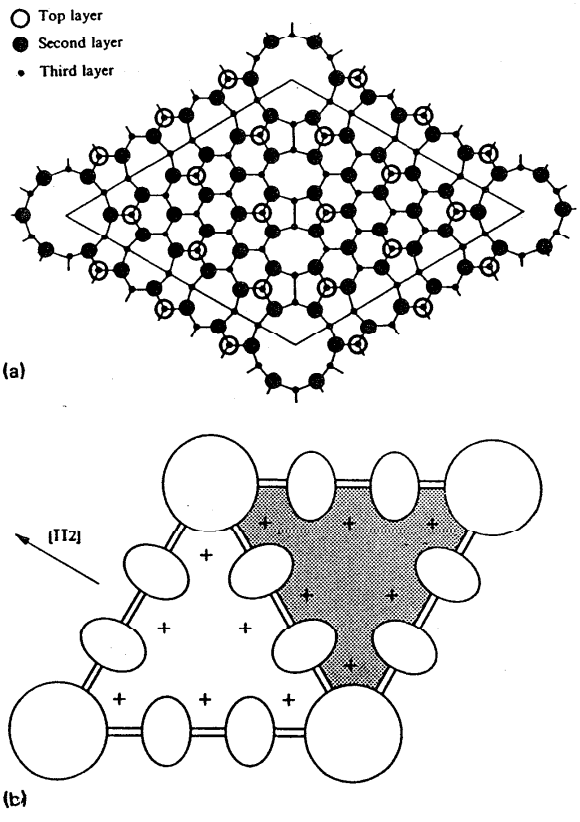

FIG. 8. Schematic diagram of the Si(111) (7×7) structure. (a) first three layers in plan view showing joining of double layers at the edge of a triangular island. Dimers are formed by pairing atoms common to each pair of 5-membered rings (Ref. 219). (b) Plan view showing the stacking fault (shaded area), prominent depressions in the surface (round and oval holes), and dimers (double lines) (Ref. 139a).

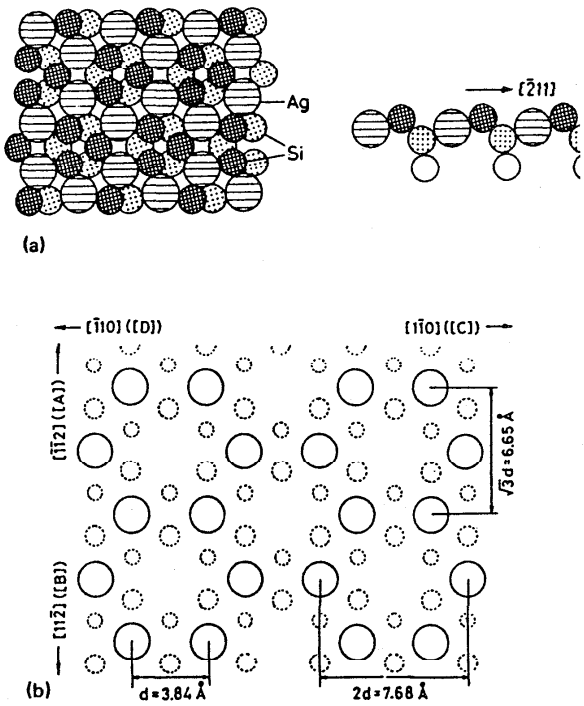

FIG. 9. (a) Model for Ag atoms embedded below topmost Si(111) layer $(\sqrt{3}\times\sqrt{3})$R30° structure (Ref. 145). (b) Model for Ag atoms adsorbed honeycomb arrangement above topmost Si(111) layer $(\sqrt{3}\times\sqrt{3})$R30° structure (Ref. 146).

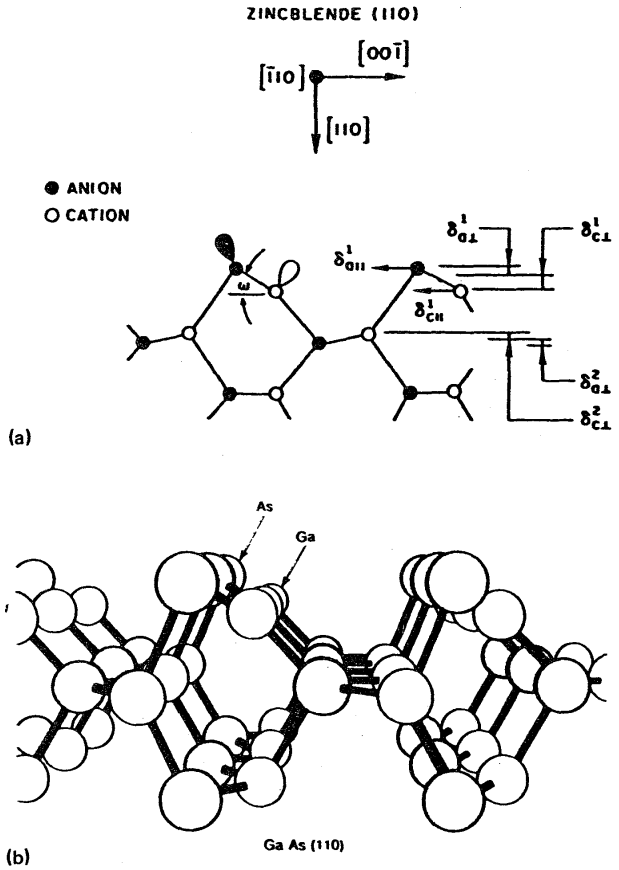

FIG. 10. (a) Schematic diagram of the relaxed zincblende (110) surface (Ref. 231). (b) View of the GaAs(110) (1×1) reconstructed surface. From (Ref. 230).

Although an early HEIS study[82] agreed with the bond relaxation 7° model, later MEIS measurements by Smit *et al.*[83] reaffirmed a bond length-conserving rotation of 29°. These authors attribute the conflict with the HEIS work to more careful surface preparation.

The bond length conserving structure for III-V (110) surfaces has been further strengthened by the finding of similar approximately 30° rotations for GaSb and InAs (see Table 10).

The GaAs(100) surface shows a large number of complex reconstructions that are dependent upon the Ga/As ratio in the surface after preparative procedures. A HEIS study[81] has indicated that the H-saturated surface relaxes to a bulk-like geometry. The same study found for the c(4×4) surface significant lateral displacements of surface Ga and As, atoms and subsurface strain.

5.4. Other Nonmetal Surfaces

The number of ion scattering studies on surfaces on nonmetals other than semiconductors are rather small, and often not very complete. They include: diamond,[61] LaB_6,[86,87] and UO_2.[162–164]

The most complete of these investigations is that of Derry *et al.* on diamond,[61] both H-terminated (1×1) and reconstructed (2×1). MEIS showed the H-terminated surface to be bulk-like and unrelaxed (within 0.05 Å), in good agreement with LEED data.[63] The scattering from the (2×1) reconstructed surface was consistent with a pi-bonded chain structure of the type seen on the equivalent Si surface.

Table 10. Atomic geometries of zincblende (110) surfaces determined by ion scattering and LEED crystallography[a].

	Layer	$\delta_{a\perp}$ (Å)	$\delta c_\perp$ (Å)	$\delta a_\parallel$ (Å)	$\delta c_\parallel$ (Å)	ω (deg)	Method	Ref.
GaAs	1	↑0.12	↓0.06	≤0.1	≤0.1	7	HEIS	82
	2	↓0.03	↑0.03	0.0	0.0		LEED	225
	1	↑0.14	↓0.51	-0.33	-0.49	27	LEED	222
	2	↓0.06	↑0.06	0.0	0.0			226
	1	↑0.20	↓0.51	-0.34	-0.51	29	MEIS	83
GaSb	1	↑0.22	↓0.55	-0.38	-0.58	30	MEIS	85
	2	0.0	0.0	0.0	0.0		LEED	227
InAs	1	↑0.22	↓0.55	-0.36	-0.57	30	MEIS	85
	1	↑0.22	↓0.56	-0.13	-0.57	31	LEED	228
	2	↓0.07	↑0.07	0.0	0.0			

[a]Parameters are defined in Figure 10.

6. Acknowledgments

The author gratefully acknowledges the help of Ms. Jill Price, and Mr. John Mischenko in locating many of the papers. This work was supported by the National Bureau of Standards Critical Compilation of Physical and Chemical Reference Data Program through Grant No. 60NANB7D0729.

7. References

[1]P. R. Watson, J. Phys. Chem. Ref. Data **16**, 953 (1987).
[2]J. F. van der Veen, Surf. Sci. Reports **5**, 199 (1985).
[3]E. Bøgh in *Channeling*, edited by D. V. Morgan, (Wiley, London, 1973).
[4]B. R. Appleton and G. Foti, "Channeling", in *Ion Beam-Handbook for Materials Analysis*, edited by J. W. Mayer and E. Rimini (Academic, New York, 1977).
[5]J. A. Davies in, *Materials Characterization Using Ion Beams*, edited by J. P. Thomas and A. Cachard (Plenum, New York, 1978), p. 405.
[6](a) L. C. Feldman, Pure and Appl. Phys. **43**, 261 (1983). (b) L. C. Feldman, Appl. Surf. Sci. **13**, 211 (1982). (c) L. C. Feldman, CRC Crit. Rev. Solid State and Mat. Sci. **10**, 143 (1981).
[7]L. C. Feldman, J. W. Mayer, and S. T. Picraux, *Materials Analysis by Ion Channeling*, (Academic, New York, 1982).
[8]L. C. Feldman and J. W. Mayer, *Fundamentals of Surface and Thin Film Analysis*, (North–Holland, New York, 1986).
[9]J. H. Barrett, Phys. Rev. **3**, 1527 (1971).
[10]Yu. V. Martynenko, Radiation Effects **20**, 211 (1973).
[11]I. Stensgaard, L. C. Feldman, and P. J. Silverman, Surf. Sci. **77**, 513 (1978).
[12]K. Kinoshita, T. Narusawa, and W. M. Gibson, Surf. Sci. **110**, 369 (1981).
[13]G. Moliere, Z. Naturforsch. **2a**, 133 (1947).
[14]D. P. Jackson, T. E. Jackman, J. A. Davies, W. N. Unertl, and P. R. Norton, Surf. Sci. **126**, 226 (1983).
[16]Y. Kuk, L. C. Feldman, and I. K Robinson, Surf. Sci. **138**, L168 (1984).
[17]Y. Kuk and L. C. Feldman, Phys. Rev. B **30**, 5811 (1984).
[18]D. L. Adams, H. B. Neilsen, J. N. Andersen, I. Stensgaard, R. Feidenhans'l, and J. E. Sørensen, Phys. Rev. Lett. **49**, 669 (1982).
[19]W. C. Turkenburg, W. Soszka, F. W. Saris, H. H. Kersten, and B. G. Colenbrander, Nucl. Instrum. Methods **132**, 587 (1976).
[20]F. W. Saris, Nucl. Instrum. Methods **194**, 625 (1982).
[21]R. M. Tromp, J. Vac. Sci. Technol. A **1**, 1047 (1983).
[22]J. F. van der Veen, R. M. Tromp, R. G. Smeenk, and F. W. Saris, Nucl. Instrum. Methods **171**, 143 (1980).
[23]R. M. Tromp and J. F. van der Veen, Surface Sci. **133**, 159 (1983).
[24]S. M. Yalisove, W. R. Graham, E. D. Adams, T. Gustafsson, and M. Copel, Surf. Sci. **174**, 400 (1986).
[25]E. Holub-Krappe, K. Horn, J. W. M. Frenken, R. L. Krans, and J. F. van der Veen, Surf. Sci. **188**, 35 (1987).
[26]T. M. Buck in *Methods of Surface Analysis*, edited by A. W. Czanderna (Elsevier, Amsterdam, 1975), p. 75.
[27]W. Heiland and E. Taglauer, Pure Appl. Phys. **43**, 237 (1983).
[28]H. Nichus, Nucl. Instrum. Methods **218**, 230 (1983).
[29]H. Niehus and G. Comsa, Surf. Sci. **140**, 18 (1984).
[30]E. Taglauer, Appl. Phys. A **38**, 161 (1985).
[31]J. W. M. Frenken, J. F. van der Veen, R. N. Barret, U. Landman, and C. L. Cleveland, Surf. Sci. **172**, 319 (1986).
[32](a) D. J. Godfrey and D. P. Woodruff, Surf. Sci. **105**, 438 (1981). (b) H. D. Hagstrum in *Inelastic Ion-Surface Collisions*, edited by N. H. Tolk, J. C. Tully, W. Heiland, and C. W. White, (Academic, New York, 1977), p. 1.
[33]E. Taglauer, W. Englert, W. Heiland, and D. P. Jackson, Phys. Rev. Lett. **45**, 740 (1980).
[34]S. H. Overbury, W. Heiland, D. M. Zehner, S. Datz, and R. S. Thoe, Surf. Sci. **109**, 239 (1981).
[35]S. B. Luitjens, A. J. Algra, and E. P. Th. M. Suurmeijer, Appl. Phys. **21**, 205 (1980).
[36]T. M. Buck, G. H. Wheatley, and D. P. Jackson, Nucl. Instrum. Methods **218**, 257 (1983).
[37]W. Eckstein, V. A. Molchanov, and H. Verbeek, Nucl. Instrum. Methods **149**, 599 (1978).
[38]J. Yarmoff, R. Blumenthal, and R. S. Williams, Nucl. Instrum. Metho **218**, 235 (1983).
[39]W. Englert, E. Taglauer, W. Heiland, and D. P. Jackson, Phys. Scr. **T** 38 (1983).
[40]M. T. Robinson and I. Torrens, Phys. Rev. B **9**, 5008 (1974).
[41]M. Aono, C. Oshima, S. Zaima, S. Otani, and Y. Ishizawa, Jap. J. Ap Phys. **20**, L829 (1981).
[42]M. Aono, Y. Hou, C. Oshima, and Y. Ishizawa, Phys. Rev. Lett. **49**, 5 (1983).
[43]R. Souda, M. Aono, C. Oshima, S. Otani, and Y. Ishikawa, Surf. Sci. **12** L236 (1983).
[44]G. Engelmann, E. Taglauer, and D. P. Jackson, Surf. Sci. **162**, 9 (1985).
[45]*Methods of Surface Analysis*, edited by A. W. Czanderna (Elsevier, An sterdam, 1975).
[46]D. Briggs and M. P. Seah, *Practical Surface Analysis by Auger and X-r Photoelectron Spectroscopy* (Wiley, New York 1983).
[47]A. Cachard and J. B. Thomas in *Materials Caracterization Using I Beams*, edited by J. P. Thomas and A. Cachard, (Plenum, New Yor 1978), p. 405.
[48]W. Heiland, F. Iberl, and E. Taglauer, Surf. Sci. **53**, 383 (1975).
[49]R. J. Culbertson, L. C. Feldman, P. J. Silverman, and H. Boehm, Phy Rev. Lett. **47**, 657 (1981).
[50]I. K. Robinson, Y. Kuk, and L. C. Feldman, Phys. Rev. B **29**, 47 (1984).
[51]S. P. Withrow, W. Heiland, D. M. Zehner, S. Datz, and R. S. Thoe, Sur Sci. **109**, 239 (1981).
[52]S. P. Withrow, J. H. Barrett, and R. J. Culbertson, Surf. Sci. **161**, 58 (1985).
[53]W. R. Graham, S. M. Yalisove, E. D. Adams, T. Gustafsson, M. Cope and E. Tornqvist, Nucl. Instrum. Methods B **16**, 383 (1986).
[54]I. Robinson, Phys. Rev. Lett. **50**, 1145 (1983).
[55]H. Hemme and W. Heiland, Nucl. Instrum. Methods B **9**, 41 (1985).
[56]M. Copel and T. Gustafsson, Phys. Rev. Lett. **57**, 723 (1986).
[57]J. Möller and H. Niehus, Surf. Sci. **166**, L111 (1986).
[58]J. Möller, K. J. Snowdon, W. Heiland, and H. Niehus, Surface Sci. **17** 475 (1986).
[59]H. Derks, H. Hemee, W. Heiland, and S. H. Overbury, Nucl. Instrum Meth. B **23**, 374 (1987).
[60]M. Copel, P. Fentner, and T. Gustafsson, J. Vac. Sci. Technol. A **5**, 74 (1987).
[61]T. E. Derry, L. Smit, and J. F. van der Veen, Surf. Sci. **167**, 502 (1986)
[62]K. C. Pandey, Phys. Rev. B **25**, 4338 (1982).
[63]W. S. Wang, J. Sokolov, F. Jona, and P. M. Marcus, Solid State Commun **41**, 191 (1982).
[64]G. W. Graham, Surf. Sci. **184**, 137 (1987).
[65]T. M. Huphens, Nucl. Instrum. Meth. B **9**, 277 (1985).
[66](a) I. Stensgaard, R. Feidenhans'l, and J. E. Sørensen, Surf. Sci. **128**, 28 (1983). (b) D. L. Adams, H. B. Nielsen, J. N. Andersen, I. Stensgaard R. Feidenhans'l, and J. E. Sørensen, Phys. Rev. Lett. **44**, 669 (1982).
[67]J. A. Yarmoff, D. M. Cye, J. H. Huang, S. Kim, and R. S. Williams, Phys Rev. B **33**, 3856 (1986).
[68]J. A. Jarmoff and R. S. Williams, Surf. Sci. **127**, 461 (1983).
[69]M. Copel, T. Gustafsson, W. R. Graham, and S. M. Yalisove, Phys. Rev B **33**, 8110 (1986).
[70]R. P. N. Bronckers and A. G. J. De Wit, Surf. Sci. **112**, 133 (1981).
[71]R. Feidenhans'l and I. Stensgaard, Surf. Sci. **133**, 453 (1983).
[72]A. G. J. De Wit, R. P. N. Bronckers, and J. M. Fluit, Surf. Sci. **82**, 17 (1979).
[73]H. Niehus, Surf. Sci. **130**, 41 (1983).
[74]A. J. Algra, S. B. Luitjens, E. P. Th. M. Suurmeijer, and A. L. Boers, Surf. Sci. **100**, 329 (1980).
[75]A. J. Algra, E. P. Th. M. Suurmeijer, and A. L. Boers, Surf. Sci. **128**, 207 (1983).
[76]J. C. Boulliard, C. Cohen, J. L. Domange, A. V. Drigo, A. L'Hoir, J. M. Moulin, and M. Sotto, Phys. Rev. B **30**, 2470 (1984).
[77]T. M. Buck and G. H. Wheatley, Phys. Rev. Lett. **51**, 43 (1983).
[78]L. Marchut, T. M. Buck, G. H. Wheatley, and C. J. McMahon, Surf. Sci. **141**, 549 (1984).
[79]J. M. van Zoest, J. M. Fluit, T. J. Vink, and B. A. van Hassel, Surf. Sci. **182**, 179 (1987).
[80]L. Marchut, T. M. Buck, C. J. McMahon, Jr., G. H. Wheatley, and W. M. Augustyniak, Surf. Sci. **180**, 252 (1987).
[81]T. Narusawa, K. L. I. Kabayashi, and H. Nakashima, Jap. J. Appl. Phys. **24**, L98 (1985).

[82](a) H-J. Gossman and W. M. Gibson, J. Vac. Sci. Technol. B **2**, 343 (1984). (b) H-J. Gossmann and W. M. Gibson, Surf. Sci. **139**, 239 (1984).
[83]L. Smit, T. E. Derry, and J. F. van der Veen, Surf. Sci. **150**, 245 (1985).
[84]L. Smit, R. M. Tromp, and J. F. van der Veen, Nucl. Inst. Methods B **2**, 322 (1984).
[85](a) L. Smit and J. F. van der Veen, Surf. Sci. **166**, 183 (1986). (b) L. Smit, R. M. Tromp, and J. F. van der Veen, Phys. Rev. B **29**, 4814 (1984). (c) L. Smit, R. M. Tromp, and J. F. van der Veen, Nucl. Inst. Methods B **2**, 322 (1984).
[86]R. Nishitani, M. Aono, T. Tanaka, C. Oshima, S. Kawai, H. Iwasaki, and S. Nakamura, Surf. Sci. **93**, 535 (1980).
[87]M. Aono, R. Nishitani, C. Oshima, T. Tanaka, E. Bannai, and S. Kawai, Surf. Sci. **86**, 631 (1979).
[88]S. H. Overbury, Surf. Sci. **175**, 123 (1986).
[89]J. W. M. Frenken, R. G. Smeenk, and J. F. van der Veen, Surf. Sci. **135**, 147 (1983).
[90](a) I. Stensgaard, Nucl. Inst. Methods B **15**, 300 (1986). (b) I. Stensgaard and F. Jakobsen, Phys. Rev. Lett. **54**, 711 (1985).
[91]K. H. Reider and H. Wilsch, Surf. Sci. **131**, 245 (1983).
[92]H. H. Brongersma and J. B. Theeten, Surf. Sci. **54**, 519 (1976).
[93]Th. Fauster, H. Durr, and D. Hartwig, Surf. Sci. **178**, 657 (1986).
[94]W. C. Turkenburg, R. G. Smeenk, and F. W. Saris, Surf. Sci. **74**, 181 (1978).
[95]J. F. van der Veen, R. G. Smeenk, R. M. Tromp, and F. W. Saris, Surf. Sci. **79**, 212 (1979).
[96]R. Feidenhans'l, J. E. Sørensen, and I. Stensgaard, Surf. Sci. **134**, 329 (1983).
[97]E. Tornqvist, E. D. Adams, M. Copel, T. Gustafsson, and W. R. Graham, J. Vac. Sci. Technol. A **2**, 939 (1984).
[98]S. M. Yalisove, W. R. Graham, E. D. Adams, M. Copel, and T. Gustafsson, Surf. Sci. **171**, 400 (1986).
[99]C. Varelas, H. D. Carstanjen, and R. Sizman, Phys. Lett. A **77**, 469 (1980).
[100]L. K. Verheij, J. A. van Den Berg, and D. G. Armour, Surf. Sci. **84**, 408 (1979).
[101]R. G. Smeenk, R. M. Tromp, and F. W. Saris, Surf. Sci. **107**, 429 (1981).
[102]M. Schuster and C. Varelas, Surf. Sci. **134**, 195 (1983).
[103]H. Niehus and G. Comsa, Surf. Sci. **151**, L171 (1985).
[104]D. J. O'Connor, Surf. Sci. **173**, 593 (1986).
[105]J. F. van der Veen, R. M. Tromp, R. G. Smeenk, and F. W. Saris, Surf. Sci. **82**, 468 (1979).
[106]T. Narusawa, W. M. Gibson, and E. Tornqvist, Surf. Sci. **114**, 331 (1982).
[107]W. Englert, W. Heiland, E. Taglauer, and D. Menzel, Surf. Sci. **83**, 243 (1979).
[108]T. Narusawa, W. M. Gibson, and E. Tornqvist, Phys. Rev. Lett. **47**, 417 (1981).
[109]S. M. Yalisove and W. R. Graham, Surf. Sci. **183**, 556 (1987).
[110]J. H. Huang, R. S. Daley, D. K. Skuh, and R. S. Williams, Surf. Sci. **186**, 115 (1987).
[111]J. M. van der Veen, J. B. Sanders, and F. W. Saris, Surf. Sci. **77**, 337 (1978).
[112]S. C. Wu, Z. Q. Wang, Y. S. Li, F. Jona, and P. M. Marcus, Solid State Commun. **57**, 687 (1986).
[113]J. W. M. Frenken, J. F. van der Veen, R. N. Barnett, U. Landman, and C. L. Cleveland, Surf. Sci. **172**, 319 (1986).
[114]H. Niehus, C. Hiller, and G. Comsa, Surf. Sci. **173**, L599 (1986).
[115]Y. Kuk, L. C. Feldman, and P. J. Silverman, Phys. Rev. Lett. **50**, 511 (1983).
[116]P. R. Norton, J. A. Davies, D. P. Jackson, and N. Matsunami, Surf. Sci. **85**, 269 (1979).
[117]J. A. Davies, T. E. Jackman, D. P. Jackson, and P. R. Norton, Surf. Sci. **109**, 20 (1981).
[118]J. A. Davies, D. P. Jackson, N. Matsunami, P. R. Norton, and J. U. Andersen, Surf. Sci. **78**, 274 (1978).
[119]H. Niehus, Surf. Sci. **145**, 407 (1984).
[120]T. E. Jackman, J. A. Davies, D. P. Jackson, W. N. Unertl, and P. R. Norton, Surf. Sci. **120**, 389 (1982).
[121]E. Bøgh and I. Stensgaard, Phys. Lett. A **65**, 257 (1978).
[122]J. A. Davies, D. P. Jackson, N. Matsunami, and P. R. Norton, Surf. Sci. **78**, 274 (1978).
[123]W. Englert, E. Taglauer, W. Heiland, and D. P. Jackson, Phys. Scr. **T6**, 38 (1983).
[124]J. A. Davies, B. R. Appleton, J. B. Mitchell, P. R. Norton, and R. L. Tapping, Nucl. Instrum. Methods **132**, 609 (1976).
[125]J. F. van der Veen, R. G. Smeenk, R. M. Tromp, and F. W. Saris, Surf. Sci. **79**, 219 (1979).
[126]B. J. J. Koeleman, S. T. de Zwart, A. L. Boers, B. Poelsma, and L. K. Verheij, Phys. Rev. Lett. **56**, 1152 (1986).
[127](a) I. Stensgaard, L. C. Feldman, and P. J. Silverman, Surf. Sci. **102**, 1 (1981). (b) L. C. Feldman, P. J. Silverman, and I. Stensgaard, Nucl. Instrum Methods **168**, 589 (1980).
[128]R. M. Tromp, R. G. Smeenk, F. W. Saris, and D. J. Chadi, Surf. Sci. **133**, 137 (1983).
[129](a) R. M. Tromp, R. G. Smeenk, and F. W. Saris, Surf. Sci. **104**, 13 (1981). (b) R. M. Tromp, R. G. Smeenk, and F. W. Saris, Phys. Rev. Lett. **46**, 939 (1981).
[130]H-S. Jin, T. Ho, and W. M. Gibson, J. Vac. Sci. Technol. A **4**, 1385 (1986).
[131]M. T. Yin and M. L. Cohen, Phys. Rev. B **24**, 2303 (1981).
[132]W. S. Yang, F. Jona, and P. M. Marcus, Phys. Rev. B **28**, 2049 (1983).
[133]R. E. Schlier and H. E. Farnsworth, J. Chem. Phys. **30**, 917 (1959).
[134](a) H. S. Jin, T. Ito, and W. M. Gibson, J. Vac. Sci. Technol. A **3**, 942 (1985). (b) T. Narusawa, K. Kinoshita, W. M. Gibson, and A. Hiraki, J. Vac. Sci. Technol. **18**, 872 (1981).
[135]R. M. Tromp, L. Smit, and J. F. van der Veen, Phys. Rev. B **30**, 6235 (1984).
[136]L. Smit, R. M. Tromp, and J. F. van der Veen, Surf. Sci. **163**, 315 (1985).
[137]R. J. Culbertson, L. C. Feldman, and P. J. Silverman, Phys. Rev. Lett. **45**, 2043 (1980).
[138]M. Aono, R. Souda, C. Oshima, and Y. Ishizawa, Phys. Rev. Lett. **51**, 801 (1983).
[139](a) E. G. McRae, Surf. Sci. **147**, 663 (1984). (b) E. G. McRae, Phys. Rev. B **28**, 2305 (1983).
[140]P. A. Bennett, L. C. Feldman, Y. Kuk, E. G. McRae, and J. E. Rowe, Phys. Rev. B **28**, 3656 (1983).
[141]R. M. Tromp, E. J. van Loenen, M. Iwami, and F. W. Saris, Solid State Commun. **44**, 971 (1982).
[142]R. M. Tromp and E. J. van Loenen, Phys. Rev. B **30**, 7352 (1984).
[143]R. M. Tromp and E. J. van Loenen, Surf. Sci. **155**, 441 (1985).
[144]M. Saitoh, F. Shoji, K. Oura, and T. Hanawa, Jap. J. Appl. Phys. **19**, L421 (1980).
[145]M. Saitoh, F. Shoji, K. Oura, and T. Hanawa, Surf. Sci. **112**, 306 (1981).
[146]T. Narusawa, W. M. Gibson, and A. Hiraki, Phys. Rev. B **24**, 4835 (1981).
[147]E. J. van Loenen, M. Iwami, R. M. Tromp, and J. F. van der Veen, Surf. Sci. **137**, 1 (1984).
[148]M. Aono, R. Souda, C. Oshima, and Y. Ishizawa, Surf. Sci. **168**, 713 (1986).
[149]H. S. Jin, A. S. Yapsir, T-M. Fu, and W. M. Gibson, Appl. Phys. Lett. **50**, 1062 (1987).
[150]K. Oura, M. Katayama, F. Shoji, and T. Hanawa, Phys. Rev. Lett. **55**, 1486 (1985).
[151]Y. Yabuuchi, F. Shoji, K. Oura, and T. Hanawa, Surf. Sci. **131**, L412 (1983).
[152]H-S. Cheng, L. Luo, M. Okamoto, T. Thundat, S. Hashimoto, and W. M. Gibson, J. Vac. Sci. Technol. A **5**, 607 (1987).
[153]S. Hashimoto, J-L. Peng, W. M. Gibson, L. J. Schowalter, and R. W. Fathauer, Appl. Phys. Lett. **47**, 1071 (1985).
[154]R. J. Culbertson, L. C. Feldman, P. J. Silverman, and R. Haight, J. Vac. Sci. Technol. **20**, 868 (1982).
[155](a) T. Narusawa and W. M. Gibson, J. Vac. Sci. Technol. **20**, 709 (1982). (b) T. Narusawa and W. M. Gibson, Phys. Rev. Lett. **47**, 1459 (1981).
[156]N. W. Cheung, R. J. Culbertson, L. C. Feldman, P. J. Silverman, K. W. West, and J. W. Mayer, Phys. Rev. Lett. **45**, 120 (1980).
[157]E. J. van Loenen, J. W. M. Frenken, J. F. van der Veen, and S. Valeri, Phys. Rev. Lett. **54**, 827 (1985).
[158](a) K. Oura, Y. Yabuuchi, F. Shoji, T. Hanawa, and S. Okada, Nucl. Inst. Methods **218**, 253 (1983). (b) Y. Yabuuchi, F. Shoji, K. Oura, T. Hanawa, Y. Kishikawa, and S. Okada, Jap. J. Appl. Phys. **21**, L752 (1982).
[159]R. M. Tromp, E. J. van Loenen, M. Iwami, R. G. Smeenk, and F. W. Saris, Surf. Sci. **124**, 1 (1983).
[160]E. J. van Loenen, A. E. M. J. Fischer, and J. F. van der Veen, Surf. Sci **155**, 65 (1985).
[161]C. Oshima, M. Aono, T. Tanaka, S. Kawai, S. Zaima, and Y. Shibata, Surf. Sci. **102**, 312 (1981).
[162]T. N. Taylor and W. P. Ellis, Surf. Sci. **107**, 249 (1981).

[163]W. P. Ellis and T. N. Taylor, Surf. Sci. **91**, 409 (1980).
[164]W. P. Ellis and T. N. Taylor, Surf. Sci. **90**, 279 (1978).
[165]L. C. Feldman, R. L. Kauffman, P. J. Silverman, R. A. Zuhr, and J. H. Barrett, Phys. Rev. Lett. **39**, 38 (1977).
[166](a) L. C. Feldman, P. J. Silverman and I. Stensgaard, Surf. Sci. **87**, 410 (1979). (b) I. Stensgaard, L. C. Feldman, and P. J. Silverman, Phys. Rev. Lett. **42**, 247 (1979).
[167]W. P. Ellis and R. R. Rye, Surf. Sci. **161**, 278 (1985).
[168]C. B. Duke, N. O. Lipari, and G. E. Laramore, J. Vac. Sci. Technol. **12**, 222 (1973).
[169]G. Gauthier, B. Aberdam, and R. Baudoing, Surf. Sci. **78**, 339 (1978).
[170]J. E. Demuth, P. M. Marcus, and D. W. Jepsen, Phys. Rev. B **11**, 1460 (1975).
[171]L. L. Kesmodel and G. A. Somorjai, Phys. Rev. B **11**, 630 (1975).
[172]L. L. Kesmodel P. C. Stair and G. A. Somorjai, Surf. Sci. **64**, 342 (1977).
[173]D. L. Adams, H. B. Nielsen, and M. A. van Hove, Phys. Rev. B **20**, 4789 (1979).
[174]M. A. van Hove and S. Y. Tong, Surf. Sci. **54**, 91 (1976).
[175]B. W. Lee, A. Ignatiev, S. Y. Tong, and M. A. van Hove, J. Vac. Sci. Technol. **14**, 291 (1977).
[176]J. Kirschner and R. Feder, Surf. Sci. **79**, 176 (1979).
[177]P. Heilmann, K. Heinz, and K. Müller, Surf. Sci. **89**, 84 (1979).
[178]L. J. Clarke and L. Morales de la Garca, Surf. Sci. **99**, 419 (1980).
[179](a) F. S. Marsh, M. K. Debe, and David A. King, J. Phys. C **13**, 2799 (1980). (b) M. K. Debe and D. A. King, J. Phys. C **10**, L303 (1977).
[180]R. Feder and J. Kirschner, Surf. Sci. **103**, 75 (1981).
[181]H. L. Davis and J. R. Noonan, Surf. Sci. **126**, 245 (1983).
[182]D. L. Adams, H. B. Nielsen, and J. N. Andersen, Surf. Sci. **128**, 294 (1983).
[183]H. L. Davis, J. R. Noonan, and L. H. Jenkins, Surf. Sci. **126**, 246 (1983).
[184]D. L. Adams, L. E. Petersen, and C. S. Sørensen, J. Phys. C **18**, 1753 (1985).
[185]Y. Gauthier, R. Baudoing, Y. Joly, C. Gaubert, and J. Rundgren, J. Phys. C **17**, 4547 (1984).
[186]M. L. Xu and S. Y. Tong, Phys. Rev. B **31**, 6332 (1985).
[187]W. Moritz and D. Wolf, Surf. Sci. **163**, L655 (1985).
[188](a) C. M. Chan and M. A. van Hove, Surf. Sci. **171**, 226 (1986). (b) C. M. Chan, M. A. van Hove, W. H. Weinberg, and E. D. Williams, Surf. Sci. **91**, 440 (1980).
[189]D. L. Adams, H. B. Neilsen, M. A. van Hove, and A. Ignatiev, Surf. Sci. **104**, 47 (1981).
[190]L. D. Marks, Phys. Rev. Lett. **51**, 1000 (1983).
[191]G. Binnig, H. Røhrer, Ch. Gerber, and E. Weibel, Surf. Sci. **131**, L379 (1983).
[192]R. A. Barker, P. J. Estrup, F. Jona, and P. M. Marcus, Solid State Commun. **25**, 375 (1978).
[193]J. A. Walker, M. K. Debe, and D. A. King, Surf. Sci. **104**, 405 (1981).
[194]E. Zanazzi, M. Maglietta, U. Bardi, F. Jona, and P. M. Marcus, J. Vac. Sci. Technol. A **1**, 7 (1983).
[195]J. H. Onuferko and D. P. Woodruff, Surf. Sci. **95**, 555 (1980).
[196]K. O. Legg, F. Jona, D. W. Jepsen, and P. M. Marcus, Phys. Rev. B **16**, 5271 (1977).
[197]P. M. Marcus, J. E. Demuth, and D. W. Jepsen, Surf. Sci. **53**, 501 (1975).
[198]S. Y. Tong and K. H. Lau, Phys. Rev. **25**, 7382 (1982).
[199]J. E. Demuth, N. J. DiNardo, and G. S. Cargill III, Phys. Rev. Lett. **50**, 1373 (1983).
[200]J. E. Demuth, D. W. Jepsen, and P. M Marcus, Phys, Rev. Lett. **32**, 1182 (1974).
[201]C. B. Duke, N. O. Lipari, and G. E. Laramore, J. Vac. Sci. Technol. 222 (1975).
[202]Y. Gauthier, D. Aberdam, and R. Baudoing, Surf. Sci. **78**, 339 (197
[203]R. Baudoing, Y. Gauthier, and Y. Joly, J. Phys. C **18**, 4061 (1985).
[204]S. J. White, D. P. Woodruff, B. W. Holland, and R. S. Zimmer, Surf. **74**, 43 (1978).
[205]F. Jona, H. D. Shih, D. W. Jepsen, and P. M. Marcus, J. Phys. C **12**, (1978).
[206]R. J. Hamers, R. M. Tromp, and J. E. Demuth, Phys. Rev. B **34**, 5 (1986).
[207]B. W. Holland, C. B. Duke, and A. Paton, Surf. Sci. **140**, L269 (198
[208]W. S. Yang, F. Jona, and P. M. Marcus, Phys. Rev. **28**, 2049 (1983
[209]D. J. Chadi, J. Vac. Sci. Technol. **16**, 1290 (1979).
[210]R. Feder, W. Mönch, and P. P. Auer, J. Phys. C **12**, L179 (1979).
[211]R. Feder, Solid State Commun. **45**, 51 (1983).
[212]D. J. Chadi, Phys. Rev. B **26**, 4762 (1982).
[213]K. C. Pandey, Phys. Rev. Lett. **47**, 1913 (1981).
[214]F. J. Himpsel, P. M. Marcus, R. M. Tromp, I. P. Batra, M. R. Cook Jona, and H. Liu, Phys. Rev. B **30**, 2257 (1984).
[215]F. J. Himpsel and I. Batra, J. Vac. Sci. Technol. A **2**, 952 (1984).
[216] D. J. Miller and D. Haneman, J. Vac. Sci. Technol. **16**, 1270 (1979
[217] K. Takayanagi, Y. Tanishiro, M. Takahashi, and S. Takahashi, J. V Sci. Technol. A **3**, 1502 (1985).
[218]G. Binning, H. Røhrer, Ch. Gerber, and E. Weibel, Phys. Rev. Lett. 120 (1983).
[219]I. K. Robinson, W. K. Waskiewicz, P. H. Fuoss, J. B. Stark, and P. Bennett, Phys. Rev. B **33**, 7013 (1986).
[220]S. Y. Tong, H. Huang, C. M. Wei, W. E. Packard, G. Glander, and M Webb, J. Vac. Sci. Technol. A **6**, 615 (1988).
[221]D. M. Zehner, J. R. Noonan, and H. F. Davis, J. Vac. Sci. Technol. 852 (1981).
[222]G. J. R. Jones and B. W. Holland, Solid State Commun. **53**, 45 (198
[223]Y. Terada, T. Yoshizuka, K. Oura, and T. Hanawa, Surf. Sci. **114**, (1982).
[224]R. J. Meyer, C. B. Duke, A. Paton, A. Kahn, E. So, J. L. Yeh, and Mark, Phys. Rev. B **19**, 5194 (1979).
[225]C. B. Duke, S. L. Richardson, A. Paton, and A. Kahn, Surf. Sci. **1** L135 (1983).
[226](a) M. W. Puga, G. Xu, and S. Y. Tong, Surf. Sci. **164**, L789 (1985). (C. B. Duke and A. Paton, Surf. Sci. **164**, L797 (1985).
[227]C. B. Duke, A. Paton, and A. Kahn, Phys. Rev. B **27**, 3436 (1983).
[228]C. B. Duke, A. Paton, and C. R. Bonapace, Phys. Rev. B **27**, 6 (1983).
[229]G. A. Somorjai and M. A. van Hove, *Adsorbed Monolayers on Surfa* (Springer–Verlag, Berlin, 1981).
[230]J. M. MacLaren, J. B. Pendry, P. J. Rous, D. K. Saldin, G. A. Somor M. A. van Hove, and D. D. Vvendensky, *Surface Crystallographic Inf mation Service: A Handbook of Surface Structures* (D. Reidel, D drecht, 1987).
[231]A. Kahn, Surf. Sci. **168**, 1 (1986).
[232]K. O. Legg, F. Jona, D. W. Jepsen, and P. M. Marcus, J. Phys. C **10**, (1977).
[233]J. W. M. Frenken, R. G. Smeenk, and J. F. van der Veen, Surf. Sci. **1** 147 (1983).
[234]T. E. Felter, R. A. Barker, and P. J. Estrup, Phys. Rev. Lett. **38**, 1 (1977).